INSTITUTO SUPERIOR TÉCNICO
Universidade Técnica de Lisboa

fMRI data analysis techniques and the self-organizing maps approach

Tiago José de Oliveira Jordão

Dissertação para a obtenção do Grau de Mestre em

Engenharia Informática e de Computadores

Presidente:	Prof. António Rito da Silva
Orientador:	Prof. Andreas Miroslaus Wichert
Vogal:	Prof. João Sanches
Vogal:	Prof. Patrícia Figueiredo

Outubro 2010

Acknowledgements

I would like to thank Prof. Andreas Wichert for always being available to answer my many questions and for our conversations that opened my eyes for a great deal of things.

My thanks to Prof. Patrcia Figueiredo and Prof. João Sanches for providing the data without which it would not be possible to perform my study.

Finally a big thank you to my parents, sister and friends for all the support and for helping me believe more in me and in my work. That made all the difference.

Abstract

Functional Magnetic Resonance Imaging (fMRI) is a widely used technique to know more about how the brain function supports mental activities. Although fMRI is a powerful tool to detect functional activation within the brain, the obtained data from fMRI experiences cannot be easily directed analyzed because of a number of factors: weakness of the signal, abundant noise in the data and the difficulty of separating activations of interest from other types. To overcome some of these difficulties powerful analysis techniques are used to interpret the fMRI data. The first part of our work will cover some of these most widely used techniques, giving a technical description of several approaches.

Our major contribution, however, will be a more detailed study of one technique in particular: the self organizing maps (SOM). To conclude about the performance of this approach we developed a data mining tool implementing the SOM algorithm and tested it with real fMRI data. In the second part of our work we will give an insight of the SOM algorithm, concluding with a presentation and discussion of our analysis results.

Keywords: Neuroimaging, fMRI, blood oxygen level-dependent signal, data analysis techniques, self-organizing maps.

Resumo

A imagiologia de ressonncia magntica funcional (fMRI) uma tcnica amplamente usada para saber mais acerca de como a funo cerebral suporta actividades mentais. Apesar da tcnica fMRI ser uma poderosa ferramenta na deteco de activao funcional ao nvel do crebro, os dados obtidos atravs de experincias, usando esta tcnica, no podem ser analisados directamente com facilidade. Factores que contribuem para esta dificuldade incluem a fraca intensidade do sinal, a abundncia de rudo nos dados e a dificuldade em separar activaes de interesse de outros tipos de activaes. Para ultrapassar algumas destas dificuldades, poderosas tcnicas de anlise so usadas para interpretar os dados de fMRI. A primeira parte do nosso trabalho vai cobrir algumas destas tcnicas, as mais aplicadas actualmente, fornecendo uma descrio tcnica para as vrias aproximaes.

A nossa maior contribuio ser, contudo, um estudo mais detalhado de uma tcnica de anlise em particular: os mapas auto-organizados (SOM). Para concluir acerca da performance desta aproximao na anlise de dados fMRI desenvolvemos uma ferramenta de minerao de dados implementando o algoritmo SOM. O algoritmo foi assim testado usando esta ferramenta com dados reais de fMRI. Na segunda parte do nosso trabalho vamos introduzir o algoritmo SOM concluindo com a apresentao e discusso dos resultados da nossa anlise.

Palavras-chave: Neuromiagiologia, fMRI, sinal BOLD, tncias de anlise de dados, mapas auto-organizados.

Contents

List of Figures

Chapter 1

Introduction

How does our brain work? This single question took a special place in that group of questions that dominates the curiosity of man since the brain was discovered as the control center of our every interaction with the world and virtually every other activity to survive. And although the question exists, there is no simple answer, because in fact the brain is still in our days the most complex machine known to man.

The complexity of the brain has been the center of many studies and experiments since remote times. Some of these early studies are dated back to 1700 BC with some manuscripts indicating that the Egyptians had some knowledge about symptoms of brain damage. Studies involving the brain are also known from ancient Greece, Roman Empire, medieval Europe, Renaissance and every other epoch and civilization throughout history. Although the advancements in technology and methodology have been helping improving our knowledge, the mechanisms of the brain are still far from being completely understood. In fact, more than ever, there is today a great scientific interest in this subject and a big community focused in solving the mysteries of the brain.

All these scientific studies involving the brain and the nervous system constitute a discipline known as neuroscience. Although neuroscience has been seen traditionally as a branch of biology it is currently defined as an interdisciplinary science that involves disciplines like mathematics, physics, medicine, psychology and computer science.

The neuroscience studies are also divided by areas of interest. Molecular, cellular and systems neuroscience are some of this areas. One of these areas is known as cognitive neuroscience and it studies the relation between cognition and the brain and how cognitive functions are produced and mapped to the neural circuitry. Here we can define cognition as a mental process involved in gaining knowledge and comprehension, including thinking, knowing, remembering, judging and problem-solving.

The cognitive neuroscience is a relatively young discipline and has been evolving with the emergence of new measurement techniques like neuroimaging combined with new sophisticated experimental techniques. Neuroimaging studies consist in the use various techniques to give us images of the structure or function of the brain. The center of our work will be around the functional magnetic resonance imaging (fMRI) technique and how it can be used to know which (and how) brain structures are activated during the performance of different tasks.

Although as we will see, fMRI is a powerful tool to detect functional activation within the brain, the obtained data from fMRI experiences cannot be easily directed analyzed. The signal is relatively weak and various sources of noise in the data must be carefully controlled. More than this the brain is constantly at work so it is not directly observable which zones of activation are related to a certain experiment. Because of these factors preprocessing steps and powerful data analysis must be applied to find task related activations within the brain.

Throughout this thesis we will give a brief insight of the fMRI technique and the principles behind it. We will also describe some important components of a fMRI experiment such as data acquisition, preprocessing and experimental design. We will then focus our attention in the data analysis step describing some of the most used techniques today applied to fMRI analysis. We will cover the statistical parametric mapping (SPM) approach, the principal and independent component analysis (PCA and ICA), the K-means and fuzzy C-means clustering algorithms. These approaches will be presented in style of a survey with a respective technical description and discussion of charecteristics and limitations to fMRI analysis.

Our major contribution, however, will be a deeper study of one analysis technique in particular called self-organizing maps (SOM). This technique is a type o artificial neural network that through unsupervised learning produces a low-dimensional representation of the data while preserving the topological properties of the input space. To better analyze the performance of the SOM approach in fMRI analysis we developed a data mining tool implementing the algorithm and tested it with real fMRI data. We will present, discuss and compare our results with those obtained using general linear model (GLM) approaches, perhaps the most used ones in fMRI analysis today.

Structure and organization of this work

This work can be roughly divided in three parts. The first one corresponds to chapter 2, where we give a brief description of the fMRI world, including history, physiological principles and typical components of an experiment. In the second part represented by chapter 3 we present in style of a survey a group of widely used techniques in fMRI analysis. Chapters 4 and 5 represent the last part of our work and refer to the SOM approach to fMRI analysis. In chapter 4 we describe the concept and algorithm and in chapter 5 we present and discuss our experimental results.

Chapter 2

Functional Magnetic Resonance Imaging

Functional magnetic resonance imaging (fMRI) is one of the most successful tools in the investigation of cognitive function, enabling brain imaging with a high spatial resolution in a non-invasive way. The acquisition of data is commonly achieved with techniques that measure the blood oxygen level-dependent (BOLD) signal changes.

The development of the BOLD contrast fMRI technique represents a considerable advancement in the area of cognitive neuroscience, but is far from giving precise responses about the mechanisms involved in the functionality of the brain. Nevertheless, a large number of experiments and studies, based on this technique, have been one of the main sources of knowledge about brain function we have today and considered an important means of knowing even more.

An fMRI experiment depends upon many factors. The experiments are composed by three main components:

- Data acquisition in scans
- Experimental tasks defined by the paradigm design
- Data analysis

All these works involve different elements and fields of expertise. From the

methods of data acquisition, preprocessing and analysis to experimental designs, analysis limitations and theories of the brain function, it is crucial the understanding of all these concepts in order to extract valid knowledge from the information obtained in fMRI studies.

In this chapter we will present an overview of the BOLD fMRI "world". We start with a brief historical introduction and description of the physiological principles behind this methodology. Next we discuss the components of an fMRI experiment, focusing on the data analysis.

2.1 fMRI - Brief history and physiological principles

Functional Brain Imaging signals measured from brain activity, namely those obtained with fMRI (functional magnetic resonance imaging) and PET (positron emission tomography), are based in local changes of blood flow (Raichle and Mintun, 2006) and metabolism (glucose utilization and oxygen consumption) (Buzsaki et al., 2007). It is known that these changes reflect and are related to cellular activity in the brain, at astrocytes and neurons level.

The idea of the relation between blood flow and brain activity is not so recent, and first came to life by the hands of an italian physiologist of the 19th century, named Angelo Mosso. Recording the pulsations of the human cortex in patients with skull defects, during mental activity, Mosso observed that these pulsations increased locally (Mosso, 1881). Nine years later, in 1890, the physiological relation between blood flow and neural activity is explored by Charles Roy and Charles Sherrington (Roy and Sherrington, 1890) setting the base theories behind fMRI. During the 20th century there were many contributions in this area, but the lack of tools to pursue these ideas was a major drawback to advancement in the beginning (for a more detailed review of the history of brain mapping see Raichle (2008).

The development of fMRI is fruit of many discoveries and work in the area during the 20th century, but we can highlight two main events: first, the emergence of the MRI (magnetic resonance imaging) technology, followed by the establishment of the basis of fMRI blood oxygen level dependent (BOLD)

by Sieji Ogawa and colleagues in 1990 (Ogawa et al., 1990a). Since then, "*fMRI has developed into the most prominent method used in functional brain imaging*"(Horwitz et al., 2000).

2.1.1 Magnetic resonance imaging

MRI is a noninvasive technique that enables the visualization and analysis of detailed internal structure of the body by producing pictures of soft tissue, organs and other internal structures. This technology is based on the fact that magnetic resonance signals are created by atomic nuclei from certain atoms (such as hydrogen, fluorine, sodium, and phosphorous) when excited by radiofrequency (RF) (van Geuns et al., 1999).

The physical principles behind MRI were discovered in 1946 by two independent groups of investigators headed by Bloch (Harvard) and by Purcell (Stanford). In their work were developed methods for determining with precision magnetic nuclear measurements (Bloch, 1946, Purcell et al., 1946). In 1973 Paul Lauterbur created a method to translate this magnetic information into cross-sectional images (Lauterbur, 1973). MRI technology uses hydrogen proton nuclei, by far the most abundant in the human body (present in great concentration in water and macromolecules), to generate the images (Sands and Levitin, 2004). The hydrogen atoms absorb energy by the form of RF pulses and re-emit it as magnetic resonance which is perceived as a small voltage in a receive coil. Two mechanisms, known as T1 and T2 relaxation, bring the hydrogen nuclei back to a relaxed state. The relaxation time depends on molecule size and binding to other molecules (McKie and Brittenden, 2005). All tissues (e.g. muscle, bone, ligaments and tendons) have different T1 and T2 relaxation times. Based on this principle, it is possible to represent the tissues with different intensities in the scan images, measuring the energy emitted by the hydrogen atoms and applying different times of detection (TE, time to echo) and repetition of the RF pulse (TR, time to repetition).

The images obtained have the advantage of having a good spatial resolution (in the millimeter scale) with a good contrast resolution (the ability to distinguish between two different tissues). There are many sources describing in much more detail the history and physical principles behind the MRI

technology. We opted for a much more simplistic perspective of MRI in order to give just an overall understanding of its mechanisms. This is important and interesting since MRI is the base of fMRI. A simple way of explaining this relation is saying that fMRI maps functionality into the brain structure obtained by MRI using the same principles of magnetic resonance.

2.1.2 Blood oxygen level dependent contrast

As already described the local changes in work flow in the human brain are directly related to brain activity. Between 1988 and 1990 a group at Massachusetts General Hospital started to experiment on the intravenous administration of MRI contrast agents in rodents (Villringer et al., 1988) and in dogs (Belliveau et al., 1990). Changes were noticed in the scans as the agent passed through the brain of the test subjects. This experiment was later made with humans and showed the same promising results (Belliveau et al., 1991). These works showed that it was possible to monitor blood flow changes in the brain using MRI, combining in one image modality, the great resolution of anatomical images of MRI with the physiology of brain function. Although the future looked promising for the area of functional brain imaging, there was still the problem of using a contrast agent that could only be administred a limited number of times. The solution to this problem was based in a study done almost half century before. During their experiments, Linus Pauling and Charles Coryell, found significant differences in magnetic susceptibilities (as much as twenty per cent) between oxygenated (arterial blood) and deoxygenated (venous blood) hemoglobin (Pauling and Coryell, 1936). Based on this discovery, it was at last the experiments preformed by Sieji Ogawa and colleagues in rodents (Ogawa et al., 1990b) that established the technique today labeled as blood oxygen level dependent contrast (BOLD contrast).

In his work Ogawa concludes that the "*deoxygenated hemoglobin in venous blood is a naturally occurring contrast agent for magnetic resonance imaging*" (Ogawa et al., 1990a). As a result of his findings he demonstrated, in vivo, images of brain microvasculature showing a contrast of the reflected blood oxygenation level. This discovery was a major step in the process of measuring activity in the brain, since neural cells increase their consumption of oxygen

when active. This consumption is compensated with increased blood flow in the areas of neural activity. Through this process, called hemodynamic response, blood oxygen is released at a greater rate to active neurons (Logothetis, 2002). Since oxygenated and deoxygenated hemoglobin have different magnetic susceptibilities, it is possible to distinguish areas with different intensities of activity. Areas with more presence of oxygen are represented in fMRI scans with more intensity (positive BOLD response), reflecting local activation.

Regarding his experiments, Ogawa, stated that BOLD contrast could be used for in vivo real time blood oxygenation brain mapping under normal physiological conditions, adding a new feature to MRI in terms of the functionality of the brain. Although BOLD contrast fMRI is not the only technique available to measure functionality with MRI technology, it is largely the most common one used in human brain imaging and therefore referred usually as the "standard" technique (Stippich, 2007).

2.2 Data acquisition

Functional activity of the brain can be observed without the use of exogenous enhancing contrast agents on a clinical strength scanner. The data acquisition typically involves a series of scans, each lasting a few seconds and covering some part or all of the brain. The obtained data from one scan is composed of several thousand points derived from a cube of brain tissue. These cubes are known as voxels and have a variable size depending on the resolution of the scanner (for a more detailed description of spatial and temporal resolution, see *Limits to the interpretation of fMRI data* on subsection 2.4). The realizable intensity and resolution vary with the magnetic field of the magnetic resonance scanners. The most broadly used are the 1.5 Tesla (T) scanners which capture about 70% of the BOLD signal, while the 1 T scanners are not suitable for BOLD analysis. High magnetic scanners (3 T or more) are also used and even permit imaging of subcortical structures (Zambreanu et al., 2005). The resulting scans are stored as a time-series (TS) of 3D volumes, where each voxel has an associated series of intensity values corresponding to the degree of activation in each scan. One aspect to retain is that each volume is not an

instantaneous picture in time. One 3D volume is the contribution of different slices recorded sequentially in different time intervals.

One other aspect of fMRI data is its richness in noise produced by several sources. These sources include thermal noise (e.g. scanner heating), power fluctuations, variation in subject cognition, head motion effects, physiological noise (induced by respiration and heart-beat) and artifact-induced problems. Performing multiple separated simulations during the fMRI experiment is mandatory, because of the low signal to noise ratio (SNR) and in order to obtain robust BOLD signals.

2.3 Paradigm design

An important factor when choosing how to analyze the data is the paradigm design where we define the "*construction, temporal structure and behavioral predictions of cognitive tasks executed by the subject during an fMRI experiment*" (Amaro Jr and Barker, 2006). In these experiments, a cognitive task is used to "provoke" the subject lying in the MRI scanner as a means to obtain a BOLD response that can identify a set of brain functions. These experiments must be done in a controlled way in order to coordinate and associate in a precise way the stimuli and the neural responses. These stimuli can be of a receptive (e.g. perception of visual or auditory material) or reactive nature (e.g. respond to a stimulus with a tap of a finger or memorize images for a certain period of time). Today there are two ways of performing cognitive studies employing fMRI: using block or event-related designs.

Block designs dominated the first years of fMRI experimentation and consist of alternative periods (30 seconds for example) that represent different cognition states. In the simplest form, the experiment is composed by two states difined by different conditions (e.g. finger taping state and resting state). In this way, it is possible to ensure that variation arising from factors not related to these states have similar impact in the signals of both states (e.g. changes in patient attention). From the signals obtained from different states it is possible to determine relative differences and identify the active neural regions that are characterized by the correspondent cognitive events.

In some cases it could be difficult to maintain a cognitive task for long periods of time, and in others the block design is not adequate (e.g. presentation of an unpredictable stimulus). In these cases an event related design can be applied using discrete repeated stimuli or responses (for reviews see D'Esposito et al. (DEsposito et al., 1999) and Rosen et al. (Rosen et al., 1998)). This type of experimental design emerged in the mid 90s making use of the faster image acquisition of fMRI. This faster acquisition enabled the detection of small changes in the hemodynamic response allowing the characterization of the BOLD signal variations and the correlation between them. In terms of the experience time, the event-related designs takes longer than the block design. Longer acquisition time is needed to achieve a sufficient signal noise ratio and longer time between stimuli is necessary to register all the hemodynamic response from one event.

2.4 Data analysis

The analysis of fMRI data has the objective to extract functional correlates from the obtained data sets (Sommer and Wichert, 2003) and identify brain regions involved in functions of interest. One of the main difficulties, when analyzing the fMRI data, is to separate the noise from the signals of interest. Other problem is the interpretation of the relation of these signals with some experimental behavior. In order to conduct the analysis of fMRI data, assumptions about the brain function must be made and sophisticated analysis techniques must be employed. In this section we will discuss the main limitations in fMRI analysis today, preprocessing techniques for enhancing the quality of the data and finally the theories of brain function behind the fMRI data analysis paradigms used today.

2.4.1 Limits to the interpretation of fMRI data

The analysis of fMRI data gives us the tools to understand the underlying neuronal activity during cognitive tasks. There are however a few limitations today that difficult the interpretation of the results from these analysis.

We start by describing the spatio-temporal limitations. In terms of spa-

tial resolution, fMRI achieves values on the scale of 2-5 mm per voxel, which offer much better resolution when comparing to other imaging techniques like EEG (electroencephalogram) and MEG (magnetoencephalogram) that measure neural activity from the brain electric and magnetic field, achieving scales of about 1 cm. Despite having a better spatial resolution, fMRI voxels are still 4-5 orders away from representing single neurons. This means that groups of neurons that can have different behaviors are grouped together in resolvable zones in the fMRI image scans.

Speaking in terms of temporal resolution, fMRI loses to the electric/magnetic methods that represent resolutions on the millisecond scale. The temporal resolution of fMRI is on the scale of seconds or even tens of seconds. In technical terms fMRI can be sampled on a millisecond scale. The limitation here is the hemodynamic response measured by the BOLD method. After the neural event there is a small dip in the blood oxygen that lags the neural response for about 1 second initially, followed by local oxygenation of the zone of activity and the respective positive BOLD signal. The peak of this response occurs only after 5-7 seconds after the initial neural event (Frahm et al., 1994).

Other main problem and focus of discussion around fMRI today is related to the question of what is really measured in terms of brain activity by analyzing the blood flow in the brain. Despite the discussion on this subject and the existence of many related studies, "*there is insufficient knowledge of the physiological basis of the fMRI signal to interpret the data confidently with respect to neural activity*" (Logothetis, 2002). Research on the matter indicates that most likely the BOLD signal reflects synaptic activity more than spike activity (Jueptner and Weiller, 1995, Mata et al., 1980), although this two physiological components are related. There are also some studies that try to show evidence of a proportional relation between the BOLD signal and the fire rates (Heeger et al., 2000).

Despite all these works, there is still not sufficient knowledge or a well established model of the relation between the hemodynamic response and neural activity. Nevertheless and ultimately, there is an agreement about the importance that a profound understanding of this relation represents for the interpretation of results obtained from BOLD fMRI (Logothetis, 2008).

2.4.2 Data preprocessing

Data preprocessing is a necessary step, in fMRI analysis, to correct non-task related variability in the experimental data. A numerous of factors explains the necessity for preprocessing. First of all, the measured BOLD signal is very small compared to the total intensity of the MR signal. Second, the task related signal change is very small compared to the total spatial and temporal variability across scans. Finally, as we have already mentioned, the signal noise ratio (SNR) is very low. Different software packages accomplish fMRI data preprocessing in different ways, although there are a set of typical steps performed when preprocessing the data.

Slice timming correction accounts for the fact that slices, that compose the total volume of the brain, are acquired at different times. Most of analysis techniques presume that every voxel is sampled exactly at the same time. Slice timing correction is particularly important when the times to repetition (TRs) are long and the expected hemodynamic response may vary significantly between slices.

Other important step is the correction of head motion. Despite the imposed physical restrictions to movement of the subject, much effort has been done also to estimate head motion to correct the data. This task is performed to guaranty that each voxel represents a unique part of the brain. One simple assumption in the estimation of motion is that the head is a rigid body (i.e. the brain and the head do not change their shape, only their position and orientation). With this assumption, estimations of the translations and rotations are done by minimizing the distance between the scanner and the target (see Brammer (2001) for an introductory review on motion correction).

Physiological noise correction can also be done. This area has not been subject of as much research as correction of head motion, because of the much subtler effects that produces. A general method for the estimation and correction of physical effects is purposed by Hu et al. (1995). The method involves the simultaneously monitoring of physiological activity and functional data, and assumes a pseudo-periodic nature of the heart beat and respiration to estimate the contribution of these effects on the data space.

Although not having the function of removing any specific noise, other

common steps in data preprocessing include co-registration, normalization and smoothing of obtained images. Co-registration is used to align the functional images with anatomical images that have better resolution, enabling the identification of the activations in the subject's individual brain. Normalization is the process of mapping the obtained image into a normalized anatomical space in order to allow a generalization of the results to a larger population. Doing this improves the comparison between other studies and subjects. Finally we have the smoothing of the data which is explained mainly by two reasons. First, smoothing may improve the SNR, since the effect is to blur the measured signal in neighboring voxels. If small amounts of smoothing are performed, the noise will get averaged, but the signal of interest should not be significantly affected (Lazar, 2008). The second reason is to improve the quality of the data for statistical analysis by making it "more normal". Despite these advantages, the size of the smoothing filter must be carefully chosen. Larger filters than some region of activity may lead to undetected activations. If too small, the filter will not improve the SNR and spatial resolution degradation will occur. Smoothing can be also the cause for some functional different areas to be merged together (Geissler et al., 2005). Some of these disadvantages are the reason why some groups do not use smoothing. A common and reasonable approach is to compare the results with and without smoothing in order to measure the influence of it in the fMRI analysis results (Lazar, 2008).

2.4.3 Theories of brain function and analysis paradigms

In order to analyze the data obtained from fMRI, it is fundamental to know what hypotheses we want to test, what comportment to explore or what to expect from neural activity. Cognitive principles defined by cognitive science are essential in the formulation of experimental designs and in the determination of what kind of data analysis strategies are best suited to analyze brain function. There are two general theories of brain function today derived from studies of neural function. The first is the notion of functional specialization (Friston, 1997a, Zeki, 1990) and the second the notion of functional integration (Friston et al., 1993, Gerstein, 1970).

Function specialization is the main assumption considered in functional

imaging studies. This theory states that stereotyped patterns are expressed by specialized cortical areas and neural populations in response to specific types of stimulus. In other words, different brain regions participate in different neural functions. This principle is well established, mainly through studies of visual neuroscience (Zeki, 1990). The functional specialization hypothesis leads to what we call the subtraction paradigm (Horwitz, 1994). This paradigm is the predominant tool in most of fMRI studies and is implemented by comparing the BOLD signals between different scans, each representing a different experimental condition. The commonly employed protocol for these studies is the block design. One simple example of the subtraction paradigm would be the comparison of two fMRI scans taken in two different experimental conditions (Posner et al., 1998). The differences in signal between the two scans determine presumably the regions involved in the two conditions. This analysis can be done using hypothesis/model driven techniques, which require prior knowledge about activation patterns. These approaches characterizations are inferential in nature and are based upon some sort of statistical parametric mapping (SPM). SPM uses voxel-specific statistics that test certain hypothesis about the dynamics of that voxel, in order to construct activation images (see subsection 2.5).

According to the functional integration theory a task represented by an experiment condition is the result of the interaction between different regions of the brain. Each different task is the result of different interaction networks. The analysis of functional integration has the objective to determine what nodes integrate these networks and how they are functionally connected. This concept supposes that localized areas are included dynamically into networks according to the cognitive tasks and that these localized areas can belong to more than one network. This assumption tells us that a brain area can have different functions.

Regarding the theory of functional integration we can analyze the problem furtherer by defining two new concepts: functional and effective connectivity. The notion of functional connectivity is a simple one. It explores a direct relation between two brain regions. In terms of data analyses this can be done by simply correlate each zone's associated time-series of neuronal activity. In the fMRI case these series corresponds to the hemodynamic response.

The analysis of these correlations is the base of the covariance paradigm (Horwitz, 1994). By analyzing the voxel's time-series correlations it is possible to infer something about the regions which are important nodes in the studied network, and how these nodes are functionally connected. Exploratory analysis techniques are used today to analyze functional connectivity. Unlike data driven techniques, exploratory/data-driven analysis do not require prior knowledge about activation patterns. In our description, we will distinguish two model-free methods: transformation-based methods (see subsection 2.7) and clustering based methods (see subsection 2.6).

The concept of effective connectivity is not so simple to define but it is closer to the intuitive notion of connection, measuring the influence one neural system exerts over another at a synaptic and cortical level (McIntosh and Gonzalez-Lima, 1994). Effective connectivity can be measured as the probability of two neurons firing together in an interval of time or as function of synaptic efficacy and contribution (Aersten and Preissl, 1991). This analysis is done with support of a casual model of the interaction between the members of the analyzed neural system. The description of causal inference analysis is out of the scope of our study (for an introduction about the concept see Pearl, 2001 (Pearl, 2001)).

As we have seen the theories of brain function are one important element on the decision of the data analysis approaches. Despite the differences between these theories and approaches, functional integration and specialization must not be seen as exclusive theories. They must be regarded as complementary and both necessary to the understanding of the data resulting from functional imaging experiences.

Chapter 3

Analysis techniques

As we already mentioned, there are today a considerable number of techniques applied to the analysis of fMRI data. These techniques, or algorithms, can be chosen taking into account the nature of the experiments, the theories of the brain function we want to test and the strengths/limitations of each approach. Besides this, is also common to observe the use of hybrid approaches and algorithm variants as a mean of overcoming some of the inherent limitations and combine in one study more than one theory of brain function. The number of papers, articles, studies and books describing this subject is so vast, that is impossible to give a complete overview of all that has been done regarding the area of fMRI analysis. Knowing this, our approach in this chapter will be to analyze some of the most used and considered algorithms. We will describe the main idea behind each algorithm, how this can be applied to the fMRI study and corresponding strengths and limitations of these approaches. For this we will divide these techniques in three groups: statistical parametric mapping, transformation based techniques and clustering based techniques. Although the self-organizing maps algorithm can be included in the clustering based techniques we will talk about it in more detail in the next chapter as this is the algorithm used in our approach.

3.1 Statistical parametric mapping

Statistical parametric mapping (SPM) (Friston, 1997b) is based on the general linear model (GLM) and is one of the commonly used approach for fMRI data analysis. SPM includes methods like ANOVA, correlation coefficients and t-tests.

In an fMRI experiment the tested data is the combination of the BOLD signal changes from experimental conditions, physiological effects and from other sources (e.g. head motion, scanner noise). The fundamental principle of SPM is that a signal depending simultaneously on these variables can be decomposed in terms of the variables contributions. This is only valid if sufficient sampling of the signals is obtained with different contributions of the independent variables. The SPM framework is composed of different modules for:

- Image preprocessing.
- Using the GLM to perform statistical tests on each voxel (univariate approach).
- Making statistical inference with distributional approximations using Gaussian Random Fields.

Image Preprocessing aims to reduce unwanted variance in the voxel time-series that results from factors like subject movement or shape differences among different scans. The preprocessing involves the following steps:

1. Realignment by correction of head motion that can cause changes in the signal intensity overtime.
2. Adjustments for movement related effects. These effects normally are the cause of about 90% of signal variance and include movement between slice acquisition, interpolation artifacts, nonlinear distortion due to magnetic field inhomogeneities and spin-excitation history effects.
3. Normalization by mapping the obtained images onto a template that conforms to a standard anatomical space.

4. Spatial Smoothing to render the errors more normal in their distribution and to permit the efficient application of the Gaussian Random Field theory.

The next step is the application of the GLM. This application requires two assumptions: independence and normal distribution of the errors terms. The center of the GLM is a simple equation that relates observations to expectations by expressing the observed response Y as a linear combination of expected components (or explanatory variables) X and an associated residual error ε:

$$Y = X\beta + \varepsilon \tag{3.1}$$

In terms of an fMRI experiment, Y represent the time-course (TC) of the voxel we want to analyze. The matrix X is called design matrix and contains the explanatory variables that represent the experimental conditions under which the observations were made. Each row of the design matrix represents a different scan and each column some effect of the experience or an effect that may confound the results. The explanatoy variables or predictors are obtained by using a box-car function with a standard time-course of the hemodynamic response. A simple condition box-car of the time-course could be defined with values of 1 when an experimental condition is verified (on) and values of 0 in other cases (off). β is the set of coefficients to be determined, relating the voxel TC values to the experimental independent variables. In other words β characterizes preference profiles of the voxel for the experimental conditions modeled in the design matrix. Finally ε is a set of random error terms conforming to a Gaussian or normal distribution. The GLM equation can be expressed using the matrix notation:

$$\begin{bmatrix} y_1 \\ \vdots \\ \vdots \\ y_n \end{bmatrix} = \begin{bmatrix} X_{1,1} & X_{1,2} & \cdots & X_{1,p} \\ X_{2,1} & X_{2,1} & \cdots & X_{2,p} \\ \vdots & \vdots & \ddots & \vdots \\ X_{n,1} & X_{n,2} & \cdots & X_{n,p} \end{bmatrix} \begin{bmatrix} \beta_1 \\ \vdots \\ \vdots \\ \beta_p \end{bmatrix} + \begin{bmatrix} \varepsilon_1 \\ \vdots \\ \vdots \\ \varepsilon_n \end{bmatrix} \tag{3.2}$$

The estimation of β and its variance are accomplished using an Ordinary Least Squares (OLS) approach, which computes the $\hat{\beta}$ (β-estimates) that minimizes

the sum of squares residuals $\varepsilon^T\varepsilon$ ($\sum_{t=1}^{N}\hat{\varepsilon}^2$):

$$\hat{\beta} = \left(X^T X\right)^{-1} X^T Y \tag{3.3}$$

$$var(\hat{\beta}) = Var(\varepsilon)(X^T X)^{-1} \tag{3.4}$$

These equations can be used in a vast range of statistical analyses. Despite this possibility the main focus here should be a good formulation of the design matrix X in order to model with a good precision the experimental design and obtain the best results from the inferences made. If the design matrix does not contain all relevant predictors, changes in the signal of the voxels will be accounted for errors instead of the model. Inferences about the contributions of the predictors to the observed signal are made using F or T statistics. This can be done by testing the null hypothesis that all the estimates are zero using the F statistic to infer about the success of the overall model in explaining the voxel TC. To infer about a combination of predictors in explaining the voxel TC, we test the null hypothesis that some linear combination of the estimates is zero using the T-statistics with $n - p$ degrees of freedom:

$$t = \frac{c^T\hat{\beta}}{\sqrt{Var(\varepsilon)c^T(X^T X)^{-1}c}} \tag{3.5}$$

Here c is the contrast vector that specifies the hypothesis we want to test. The denominator of the function defines the standard error of $c^T\hat{\beta}$, i.e. the variability of the estimate due to noise fluctuations. In one case, for example to test weather activation in condition 1 is significantly different form activation in condition 2 of the experience, by the null hypothesis we would have $H_0 : \hat{\beta}_1 = \hat{\beta}_2$ or $H_0 : (+1)\hat{\beta}_1 + (-1)\hat{\beta}_2 = 0$. The values used to multiply the β-estimates values are the contrast vector. In this case we would have $c = [1, -1]$.

With the known degrees of freedom a t value for a specific c contrast can be converted into an error probability p (probability of obtaining the observed effect, quantified by the T statistic, due solely to noise fluctuations). These tests are performed for every voxel with the same contrast vector c and the $\hat{\beta}$ of each voxel. The correspondent t and p values are then saved on a statistical map in the position of each voxel. Voxels exceeding a specified statistical

threshold are visualized in the final image with different intensities or colors (to distinguish from anatomical information) according to their contribution to the studied signal.

The specification of an appropriate threshold for the statistical maps represents a main issue here. A conventional threshold with a probability $p < 0.05$ would mean that in 100 voxels we would wrongly declare an average of 5 when they have no effect on the modulated condition. With the analysis of 100,000 voxels we would have an average of 5,000 false positives (Type I errors). One way to resolve this problem is the application of the Gaussian Random Fields theory. The GRF provides a way of adjusting the p values by taking into account the fact the neighboring voxels are not independent by virtue of continuity in the original data. The discussion of the GRF is out of the scope of our review (for more detailed information on this matter or on the SPM method see Friston et al. (1995)).

Methods based on the general linear model, like SPM, are currently one of the most used analysis strategies. One of the reasons is that the method offers an intuitive approach to the analysis of fMRI. On the other side these approaches are based on a set of tenuous assumptions. The first is that the observations have a known distribution (e.g. Gaussian). Second SPM assumes that the time-course of different sources can be reliably estimated in advance. This involves fitting the acquired data into a canonical hemodynamic response function, making an assumption about the temporal evolution of the fMRI data. The third assumption is that the variances and convariances of the BOLD signal between repeated measurements are equal. The last assumption is that the signals at different voxels are considered independent. All these assumptions can lead to invalid or inefficient statistical tests. Finally, one other thing to take into account when using SPM is that it relies on smoothing of the data, which may degrade the inherently good spatial resolution offered by fMRI.

3.2 Transformation-based analysis

The transformation based methods transform original data into a high-dimensional vector space in order to separate different functional responses and types of noise from each other. The new vector space will be composed of several components, each one representing typical spatial or temporal responses of functional activity and various noise sources. There are two transformation-based methods applied to fMRI: principal component analysis (PCA) and independent component analysis (ICA). Both methods use a transformation matrix to remove diffuse and complex patterns of correlation between the element vectors of the original data. PCA uses only second-order statistics and decorrelates the outputs using an orthogonal matrix. ICA attempts to make the outputs as statistically independent as possible while placing no constraints on the transformation matrix.

3.2.1 Principal component analysis

Principal component analysis (PCA) is a popular analysis tool actively used in fMRI studies (Hansen et al., 1999, Lai and Fang, 1999, Viviani et al., 2005, Suma and Murali, 2007, Andersen et al., 1999) with the assumption that fMRI data has high variability. The PCA method decomposes the data obtained, into sets that describe uncorrelated event sequences in the original data. This is done through the identification of principal components that individuate important variations in high dimensional data as a set of orthogonal directions in space (Jolliffe, 2002). Furthermore the principal components obtained through PCA are ranked according its contribution to the variability of the data, giving the means to capture the most important and significant variations in fMRI sets.

PCA provides a simplified representation of the data by projecting the data vector onto a set of eigenvectors and generating a new feature space of principal components. The eigenvectors are extracted from the estimated covariance matrix of the data. Most often, by discarding low-variance components (with lower eigenvalues), the dimensionality of the data will also be reduced.

Let X be the fMRI data matrix $M \times N$, with zero empirical mean (the empirical mean of the distribution has been subtracted from the data set), where N is the number of column vectors in the data set and M is the number of elements in each column vector (dimension). The PCA method is used to generate a new feature space Y using the following equation:

$$Y^T = X^T W \tag{3.6}$$

where W is the $M \times P$ matrix of basic column vectors composed by a set of P eigenvectors from the $M \times M$ covariance matrix C of the data.

Two analyses of fMRI data can be made using the PCA. In one, the data matrix has dimension $n \times p$, with n being the number of time-points (number of scans) and p the number of voxels. The covariance matrix will be of dimension $n \times n$. This matrix reports on the temporal covariance structure. In the data matrix X, each time-point will be interpreted as a random variable, and the voxels will represent repeated observations of the temporal response. The principle components of the new feature space will be vectors representing all voxels and their respective activation values. In the second case we will have a data matrix of dimension $p \times n$ and a covariance matrix of dimension $p \times p$, which will report directly on the spatial covariance structure. In this case, each voxel in the data matrix X will be a random variable, and the separate rows for each time-course will represent repeated observations of a stationary random process. The principal components of this second analysis will be vectors representing different typical TCs. In either of the cases the covariance matrix in matrix notation can be represented as:

$$C = \begin{pmatrix} cov(X_1, X_1) & cov(X_2, X_1) & \cdots & cov(X_1, X_j) \\ cov(X_2, X_1) & cov(X_2, X_2) & \cdots & cov(X_2, X_j) \\ \vdots & \vdots & \ddots & \vdots \\ cov(X_i, X_1) & cov(X_i, X_2) & \cdots & cov(X_i, X_j) \end{pmatrix} \tag{3.7}$$

where X_i is a random variable and $cov(Xi, Xj)$ is the covariance between variable X_i and X_j:

$$cov(X_i, X_j) = \frac{\sum_{k=1}^{n} X_{ik} X_{jk}}{n} - \bar{X}_i \bar{X}_j \tag{3.8}$$

The next step would be to find the eigenvectors of the covariance matrix C. Only square matrices have eigenvectors, but not all of them. If a matrix

$n \times n$ has eigenvectors it will have n of them. The eigenvectors of a matrix will all be orthogonal between them ensuring the uniqueness of all principal components. First we need to find the eigenvalues of C given by the following equation:

$$det(C - \lambda I) = 0 \tag{3.9}$$

where I is the identity matrix and λ is the variable we want to compute (the eigenvalues). The first principal component will correspond to the linear combination of variables with maximum variance, and will be the projection of the data onto the eigenvector with the highest eigenvalue. The second principal component will have the second largest variability and will be the projection onto the eigenvector with second highest eignevalue and so on. Like we said all principal components will also be orthogonal between them. Knowing this is important to sort the eigenvalues in order to find the most significant principal components. The eigenvectors are calculated solving the following equation:

$$CE = \lambda E \tag{3.10}$$

Where E is the column eigenvector we want to calculate, C is the covariance matrix of the data and λ is the selected eigenvalue. The matrix W (eq. 16) will be composed of eigenvectors, and will be the transformation matrix of the data into the new feature space. Reduction of the dimension of the data can be accomplished by selecting only the eigenvectors with highest eigenvalues to incorporate W. There are a number of neural network architectures that can estimate principal components without calculating the covariance matrix (Oja, 1989) (Diamantaras and Kung, 1996). Also selecting the number of optimal principal components is a largely unsolved problem, with multiple purposed heuristics and statistical tests (Jackson, 1991).

One of the main problems when using PCA for fMRI analysis is the difficulty to capture small changes in signal variance related to some task related experiences. This happens because the principal components are projected onto orthogonal eigenvectors that express only the greatest variance in the data. The orthogonality between the principal components is also the cause of other limitation. If the signals of interest and the signals from other artifacts, such scanner or physiological noise, are non-orthogonal, this will result in loss

of important signal. Finally this approach based on voxel-pair covariance will certainly miss some overall patterns of association (e.g. some voxels becoming simultaneously activated during an experiment).

3.2.2 Independent component analysis

Independent Component Analysis (ICA) for fMRI data analysis was first introduced by McKeown et al. (1998a) and has been used in several studies to characterize brain function (Moritz et al., 2000, Duannb et al., 2000, Jung et al., 2001). The method was originally proposed to solve the blind source separation problem (e.g. recover x mixed voice signals (sources), recorded from y microphones (observations), i.e. the cocktail-party problem).

The application of ICA in fMRI analysis can be done in two ways: to separate temporally (Biswal and Ulmer, 1999, Makeig et al., 1997) or spatially independent sources (McKeown et al., 1998a). Suppose X is an fMRI data matrix $N \times M$, where N is the number of time-points of each voxel's time-course (TC) and M is the number of voxels. In temporal ICA (tICA) we consider the signals as N individual TCs and M observations. In Spatial ICA (sICA) the signals are the M voxels and there are N different observations. When studying fMRI data, sICA is more used, mainly because the spatial dimension is much larger than the temporal dimension ($M >> N$). This factor makes tICA typically much more computationally demanding (Calhoun et al., 2001) in fMRI analysis. For this reason we will discuss the sICA approach.

The application of sICA to fMRI starts by suggesting that local areas of the brain activated by performance of a psychomotor task should not be related to other areas which present signals derived from artifacts, such machine noise, physiological noise or head movement. Each of these different processes may be represented by one or more spatially independent components, each one with a single associated activity time-course and component map (the weight for each voxel)(Fig. 1).

Let us suppose that we have t (time-points) observations of $\{x_1, \cdots, x_t\}$ variables that represent the activation map of the voxels in each scan t. These variables can be modeled as a linear combination of t independent components

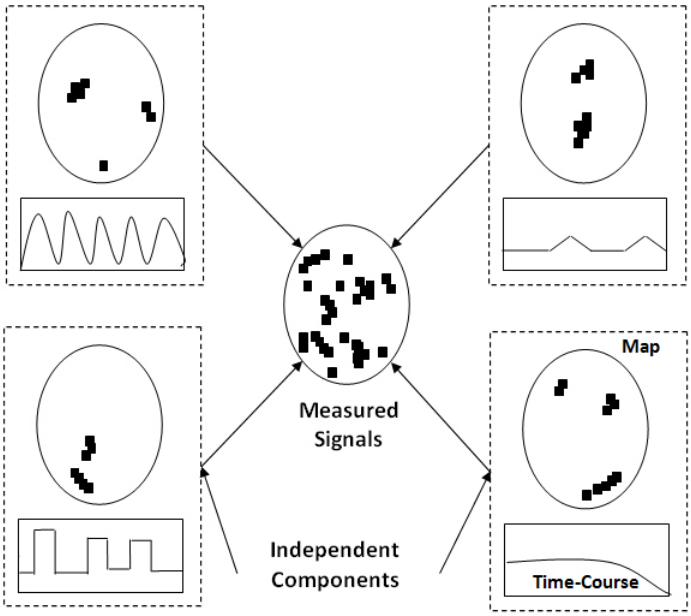

Figure 3.1: fMRI data decomposed into independent components, with associated spatial distribution of voxels and time-course.

$\{c_1, \cdots, c_t\}$:

$$x_i = m_{i1}c_1 + m_{i2}c_2 + \cdots + m_{it}c_t \tag{3.11}$$

for all $i = \{1, \cdots, t\}$, where m_{ij}, $i, j = \{1, \cdots, t\}$ are some real coefficients. By definition all components c_t are statistically independent. Using matrix notation this equation can be expressed as:

$$X = MC \tag{3.12}$$

where X is the matrix t (time-points) $\times$ n (voxels) of observed data, M is the c (components) $\times$ t mixing matrix and C is the $c \times n$ component matrix (Fig. 2). We can only observe the variables in X and must estimate M and C using X. As we can see the ICA method can extract a number of independent components up to the number of time-point present in the data. One important thing to retain from this model is that it assumes the components in the matrix C are statistically independent and have non-Gaussian distribution. Under

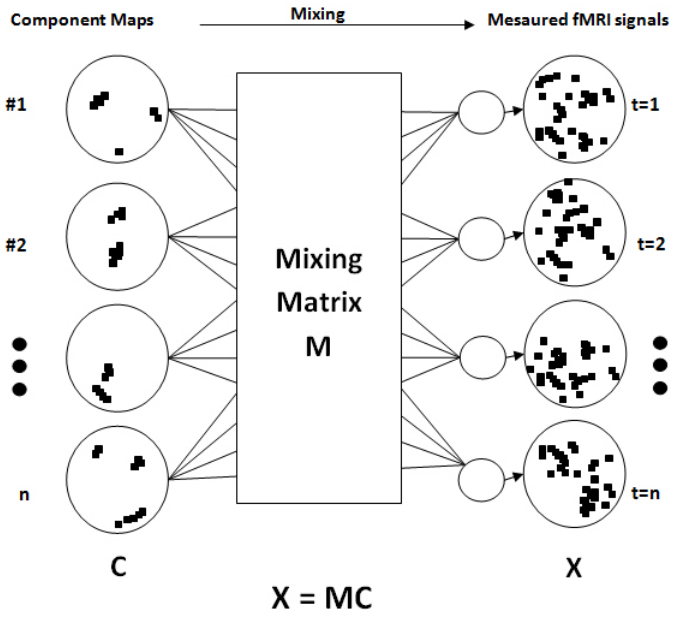

Figure 3.2: fMRI data as a mixture of independent components, where M specifies the relative contribution of each component at each time-point t.

these assumptions we can compute M and its inverse M^{-1}, the "*unmixing*" matrix. The independent components matrix C is then simply obtained with:

$$C = M^{-1}X \tag{3.13}$$

There are many approaches used for estimating M (e.g maximization of non-Gaussianity, maximum likelihood estimation, minimization of mutual information, tensorial methods) (Hyvrinen and Oja, 2000) using different algorithms (e.g. informax, FastICA, JADE). Also, one common procedure before the calculation is to first reduce the data to a linear subspace using principal component analysis (PCA) (McKeown and Sejnowski, 1998). This happens because experiments using fMRI can achieve numbers in the order of the thousands time-points, which may greatly exceed the dimensionality of the data. The number of components needed to adequately repesent the data is much smaller than this dimension (Jackson, 1991). The ICA algorithms are out of the scope of our discussion.

In terms of the significance of the results, each obtained component is

composed of n values representing the state of activation for each voxel. The distributions of these values in the component matrix C are as statistically independent as possible, while the time-courses contained in M^{-1} may be correlated. The independence is assumed if most of the voxels are sparse and non-overlapping (McKeown et al., 1998b), although some overlap will occur. Each voxel's value represents the amount a given voxel is modulated by the activation of the component. One common procedure is to use z-tests to find and display significantly contributing voxels in each component. Values greater than a certain threshold represent "active" voxels, and negative values represent voxels with opposite modulation to the time-course. In this case the z-tests have a descriptive objective rather than a statistical interpretation. When choosing the components that better describe an fMRI experiment, one can calculate the correlation between the components TCs and a modeled TC that describe the stimulus presentation, and find most significantly stimulus correlated components. Unlike the PCA approach, rank ordering the components is complicated given that the time-courses in M^{-1} are in general non-orthogonal, and so the variances explained by each component will not sum to the variance of the original data. Still there are a number of ways one can estimate the contribution of each component (e.g. using root mean square of the reconstructed data solely from the tested component (McKeown et al., 1998a)).

The analysis of fMRI data with the ICA approach has some pros and cons. The spatial division of the data into non-overlapping and specific sets provides a very nice method to identify spatial nodes that are independent and sparse. The correlation between time-courses of different components removes the constraint that artifacts non-related to the experiment have to be orthogonal to those derived from the experiment (in fMRI analyses any confounding between signals of interest and artifacts means loss of signal) (Friston, 1998). One weakness of this approach is that the attempt to find maps that are maximally independent tends to fragment some broad areas of activation into multiple maps with all having strong correlated TCs. The ICA approach difficults the identification of non-linear activation relationships between active areas, which is an important issue regarding the theory of functional integration of the brain.

3.3 Clustering-based analysis

Clustering algorithms attempt to classify the time-course (TC) signals of the voxels into several patterns according to the similarity among them. This information is organized in clusters and is independent of their spatial neighborhood. These clusters can be described by an average TC or a cluster center obtained by averaging all the TCs of the cluster in question. The resultant output maps can be calculated by labeling the pixels of the same cluster (membership map) or by plotting the distance of the TCs to a given cluster center (distance map). Clustering in fMRI can be achieved with various approximations like some of the most popular in fMRI analysis: k-means (Ding et al., 1994, 1996), fuzzy clustering (Golay et al., 1998, Scarth et al., 1995), self-organized maps (SOM) (Fischer and Hennig, 1999, Ngan and Hu, 1999) and hierarchical clustering (Goutte et al., 1999) . There are also hybrid approaches that combine different clustering techniques like k-means with hierarchical clustering (Filzmoser et al., 1999) or self-organizing maps with c-means fuzzy clustering (Chuang et al., 1999). While an extensive approach to all algorithms and all variants would be interesting, the space limitations of our document demand a less detailed review. We will focus our discussion on the principles of the k-means, fuzzing clustering, and later in the next chapter, on the self-organizing maps, pheraps the most popular clustering techniques on the field of fMRI analysis.

3.3.1 K-means clustering

The k-means algorithm is a classic statistical clustering method. The algorithm is computed in an off-line mode and does not perform competitive learning like other variants such self-organizing maps. In the k-means case all clusters centers updates are based on the training sample.

To understand its mechanisms we start by introducing a number of useful quantities. Let the set $\{x_j\}$ be composed of N vectors from $\Re^i$ where each vector corresponds to a voxels time-course (TC) and i is the number of images taken by the MRI scanner. Next we consider K clusters, and their respective center $c_k \in \Re^i$ and $1 \leq k \leq K$. The data is partitioned by clusters such each

x_j (voxel's TC) is assigned to exactly one cluster C_k. The clustering algorithm objective is this assignment while minimizing an objective function to give the low-dimensional approximation to the data. We consider two objective functions, one that calculates the within-class inertia (averaged squared distance from the TC to the cluster center) resulting from partition:

$$I_w = \frac{1}{N} \sum_{k=1}^{K} \sum_{x_j \in C_k} d^2(x_j, c_k), K \leq N \tag{3.14}$$

And other that gives the inertia between-class (averaged squared distance from the cluster center to the center of gravity):

$$I_B = \frac{1}{N} \sum_{k=1}^{K} C_k * d^2(c_k, \bar{c}), K \leq N \tag{3.15}$$

where d^2 is the squared distance of two vectors, C_k represents the number of elements in the respective cluster and $\bar{c}$ is the weighted average of all the cluster centers. The distance d is typically the Euclidean but other types are also used.

A good approach in the clustering algorithms would be minimizing the first function (eq. 6) while maximizing the inertia between clusters (eq. 7) in order to gather in one cluster TCs with much similarity as possible while maintaining considerable and notable differences from other clusters. The within-class equation is minimized when the cluster center is the average of all members of the cluster:

$$c_k = \frac{1}{C_k} \sum_{x_j \in C_k} x_j \tag{3.16}$$

In these conditions the average cluster center is also the average of the data and in other words the center of gravity. The Huygen's equation states that the sum of within-class and between-class is constant and equal to the total variance of data, regardless the number of clusters. By this principle we can assume that minimizing I_W or maximizing I_B produces the same results. . Conclusively the within-class inertia alone provides a good way to classify the quality of the partitioned data into K clusters. The values returned from it are always higher for partitions with fewer clusters, if the partitioning tasks

are made in an optimal way. I_W is therefore globally minimized if there are as much partitions as there are data vectors.

The k-means algorithm is based on the stated considerations and its objective, for K clusters, is to iteratively minimize I_W by assigning the TC vectors to the nearest cluster center and updating its value. One important thing here is that the number of clusters has to be selected before the calculations. The algorithm steps are enumerated below:

1. Start by initializing C that will contain K cluster centers $c_k \in \Re^i$ such that $1 \leq K \leq N$. The set $C = \{c_1, c_2, \cdots, c_k\}$ will be initialized with TCs x_j randomly chosen from the data set. Set iteration value to 0.

2. Assign each TC x_j from the data set to the nearest center c_k using the distance metric, $d(x_j, c_k)$.

3. Update the new cluster centers c_k with the average value of its members (eq. 8).

4. Increment iteration value. Repeat steps 2 and 3 if any partition was modified since last iteration.

The convergence of the k-means algorithm is proven and is usually very fast. In terms of an fMRI analysis the center c_k of each cluster would represent the typical TC of the voxel's inside this group.

The results of this approach depend largely on a number of factors. The number of clusters must be specified before the algorithm and a choice that does not reflect the data structure will result in weak or meaningless results. Regardless the existence or not of structure the algorithm will perform data partitioning. This makes the validation of the results necessary. One other question to address is the existence of several distance functions, like Euclidean, Manhattan and Hamming distance. The choice of the distance d metric will also have a deep influence on the results. The use of the distance function also demands pre-processing of the data (Somorjai et al., 2003). As it is the partitioning is based on the average of the TC signals. Normally this is not the objective since what is wanted is to gather in one cluster TCs with similar waveforms (temporal profiles). The use of raw inputs based on the

distance metric will merely segment the brain (Scarth et al., 1995). The final factor to consider is that the k-means algorithm is non-deterministic and the results are dependent of the cluster initialization. To overcome this difficult one can perform the algorithm several times and choose the best results based on minimum within-class inertia.

3.3.2 Fuzzy C-means clustering

The main difference between the k-means clustering and fuzzy clustering is the type of membership classification. While the "crisp" algorithm (k-means) classifies the voxels TCs as being a part of a cluster or not (1 if member of a cluster, 0 if not), the fuzzy variant separates them on a finer manner, and probably more appropriate in biological systems, with TCs being able to belong to more than one cluster with a certain degree of membership (float values between 0 and 1 depending on the degree of membership). There is more than one fuzzy clustering method. Fuzzy c-means (FCM) is one of the most wildly used and was implemented in the software package EvIdent® (EVentIDENTification) and in several studies (Baumgartner et al., 1997, Scarth et al., 1995, Baumgartner et al., 2000, Somorjai et al., 2003) with good results in analyzing brain fMRI data. We will then focus our discussion in the c-means variant.

Like k-means clustering c-means is an off-line method as opposed to other fuzzy clustering variants like Unsupervised Fuzzy Competitive Learning. Given the same quantities of the k-means method we want to obtain a pre-selected K number of partitions such each one minimizes the objective function:

$$J_m = \sum_{j=1}^{N}\sum_{k=1}^{K}(u_{kj})^m d^2(x_j, c_k), K \leq N, m \in [1, +\infty[\tag{3.17}$$

where $\{u_{kj}\}$ is the $K \times N$ cluster membership matrix in which u_{kj} is the degree of membership of jth TC x_j in the kth cluster; $m \in \Re$ is the factor that controls the "fuzziness" of the algorithm. The minimization of J_m is only obtained if:

$$u_{kj} = (\sum_{l=1}^{K}(d(x_j, c_k)/d(x_j, c_l))^{2/m-1})^{-1} \tag{3.18}$$

and

$$c_k = (\sum_{j=1}^{N}(u_{kj})^m x_j)(\sum_{j=1}^{N}(u_{kj})^m)^{-1}, 1 \leq k \leq K \tag{3.19}$$

The fuzzy C-means algorithm iterates on these two functions according to the following steps:

1. Fix the number of cluster K ($2 \leq K \leq N$) and the fuzzy index m ($1 \leq m \leq +\infty$). Set iteration t counter to zero and initialize the cluster centers $\{c_k\}$ with random TCs x_j from the data sample. Choose distance metric d.

2. Calculate the cluster centers $\{c_k\}$ (eq. 11).

3. Update $\{u_{kj}\}$ with equation 10 and $\{c_k\}$.

4. Compare $\{u_{kj}\}^{t+1}$ and $\{u_{kj}\}^t$ using a matrix norm: if $\|\{u_{kj}\}^{t+1} - \{u_{kj}\}^t\| < \varepsilon$ stop, else $t = t + 1$ and go to step 2.

Unlike the "crisp" version (k-means), the fuzzy c-means algorithm seems to be much less prone to converge prematurely to an unsatisfactory minimum of the objective function (Geva and Kerem, 1998, Gordon and Somorjai, 1992). This factor gives fuzzy c-means a definitive advantage over k-means. Also as we said earlier the classification of TCs in a finer manner than the strict classification of k-means, seems to be more appropriate to describe biological systems. Besides these advantage factors, c-means has to face much of the same problems of k-means: the dependency on a number of factors (number of clusters, distance metric), the non-deterministic nature of the algorithm, the validation of the clusters and the fact that the partition reflects more an average distance of the TCs rather than a similarity of the waveforms. There are a number of approaches when using fuzzy c-means that try to overcome these difficulties. One interesting review of Somorjai and Jarmasz (Somorjai et al., 2003) details a number of strategies and tactics on the analysis of fMRI data when using fuzzy clustering. Besides the main algorithm, the process includes image preprocessing (with noise reduction, normalization), initial partition of TCs and significance tests.

Chapter 4

Self-organizing maps

The self organizing maps (SOM) approach to fMRI analysis is a clustering type algorithm and represents the focus of our work. As such, we will get into a more detailed description comparing to the other approaches already covered. As we mentioned previously this approach was already applied in fMRI studies (Fischer and Hennig, 1999, Ngan and Hu, 1999, Peltier et al., 2003) with some interesting and promising results.

For a better understanding we opted for a slightly different approach in describing SOM in comparison with the previously covered algorithms. We divided this chapter in two parts. In the first we talk about the concept behind the algorithm. Also in this section we will complement our description with a good number of visual examples, since in our opinion this offers a great way to understand the idea behind the SOM in an intuitive manner. In the second part we describe in a more technical way the algorithm, covering each step in detail and talking about some variations of its implementation.

4.1 The Concept

The self-organizing maps (SOM) algorithm introduced by Kohonen (Kohonen, 1995) is an analog, in this case ironically, to the human brain way of organizing information in a logical manner. It is theorized that cognitive cells in the human brain, like the ones in the visual cortex, are trained in a supervised manner, while others function in a self-organized unsupervised manner. These

cells are organized topologically in a way such adjacent areas perform related cognitive functions. The SOM method emulates this unsupervised learning. In terms of the algorithm it tries to reveal structure to the data by bringing together characteristics of two other algorithms. Kohonen's maps do not partition the data into independent subsets but model its interrelation, like cluster algorithms, while performing in it a lower-dimensional projection like topological preserving mapping algorithms. The SOM approach differs from cluster approaches in the way that accounts for the neighborhood of cluster centers. One interesting thing in its use is that addresses some difficulties of the conventional clustering:

- The choice of the number of expected clusters.
- The clusters validity.
- The detection of small and large clusters within the same data set.

Kohonen's maps consist of one layer of neurons (neuron map), usually a two-dimensional grid, and each neuron has a feature array. Each neuron in the map is a cluster center and has as many input connections as the data-samples that will be used in the map training (Figure 4.1).

One good and common example of the SOM algorithm results is given in Figure 4.2. In this example the map and data set are composed initially of 10000 random colors, a 100x100 map with 10000 neurons. As we use the SOM algorithm and "feed" the data into the map we observe that, it is organized so that similar colors stay near each other, revealing structure to the data. As we said each neuron in the map has a feature array, which in this case is a three dimensional one. Each color is a contribution of three values, an amount of red, green and blue (RGB array). If we had plot these values instead of showing the resultant colors we would had a map like in Figure 4.3. Although not so evident, the organization of the data is perceptible, as similar arrays stay close to each other. Talking about the fMRI analysis case these arrays will be the voxel's time-course (TC). The training procedure is performed in several steps and has the objective of organize the TCs such that similar ones are close to each other. In the previous examples there isn't actually a reduction of the dimension of the data, since the dimension of the input is the same as the

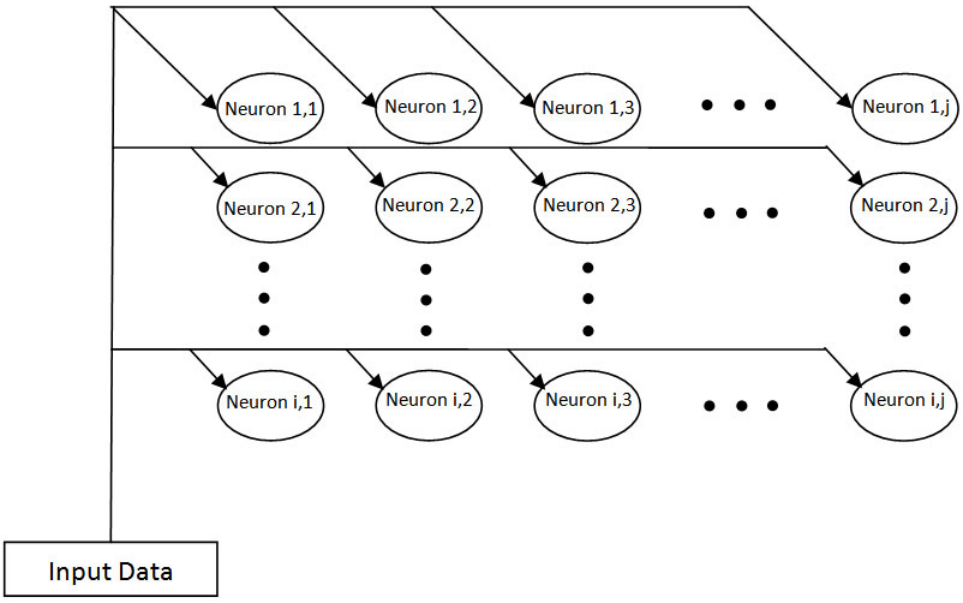

Figure 4.1: Input to 2-Dimensional neuronal topology.

dimension of the map. In the case of the fMRI analysis we will have many thousands of voxels and self-organized maps of a much lower dimension. In a 10x10 map for example we will have only 100 neurons or clusters that will be representative of all the TCs of these thousands of voxels (see Figure. 4.4). In the end, by reprojecting the obtained clusters into the anatomical space of the brain, we can identify areas with similar TCs and similar behavior (see Figure 4.5).

4.2 The algorithm

The main idea of the SOM algorithm, like we already said, is to organize data in a logical way while performing a reduction of the data dimension. We can define the algorithm as a group of typical steps in pseudo code:

1. Initialization.

2. Selection of a TC from the data set.

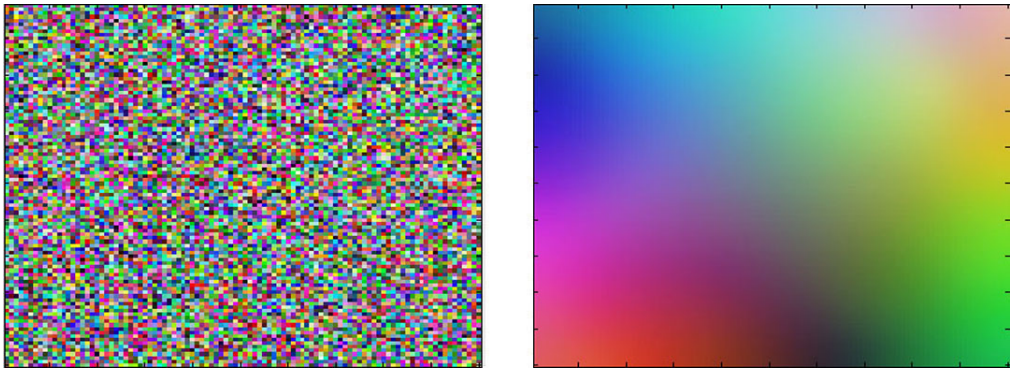

Figure 4.2: Organized colors after the application of the SOM algorithm.

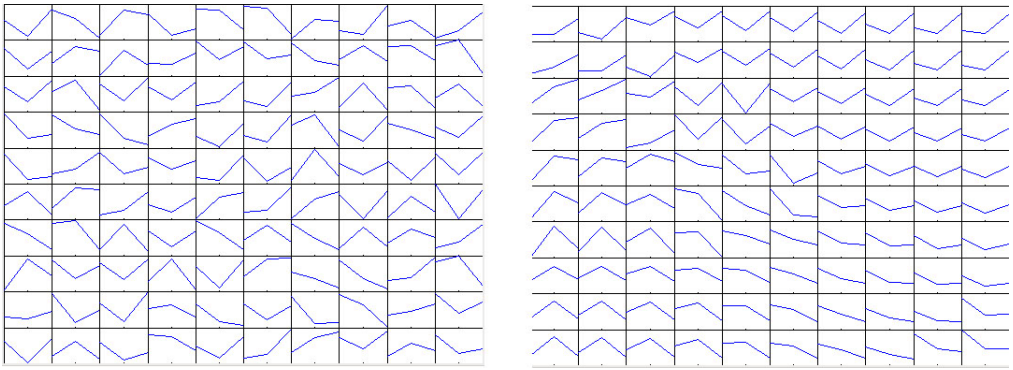

Figure 4.3: Organized RGB arrays after the application of the SOM algorithm.

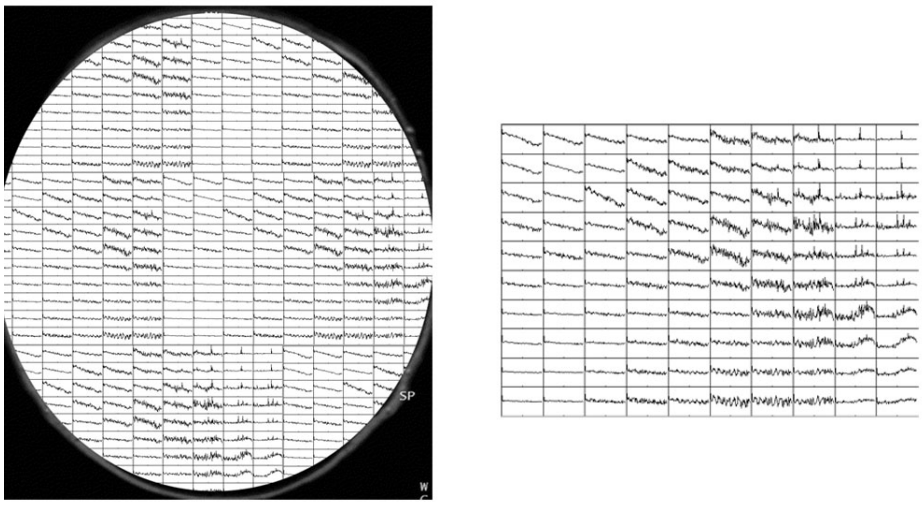

Figure 4.4: Organized TCs arrays of a slice of a brain volume with reduction of dimensionality.

3. Finding the neuron, or cluster center, of the map with minimal distance to the chosen TC.
4. Moving this neuron towards the previous TC, as well as the cluster center neighbors.
5. Updating parameters values.
6. Repeat from step 2 until stopping criteria is satisfied.

4.2.1 Initialization

This step consists of fixing the map dimension, as well as the initial parameters values. In this phase we also initialize the values of the arrays in the map. The parameters used by the algorithm are the learning rate and the neighborhood width. The first is a value that ranges from 0 to 1 and defines how much a cluster center will learn from the data. The second value corresponds to the width of a neighborhood function which determines the radius of influence of the learning process.

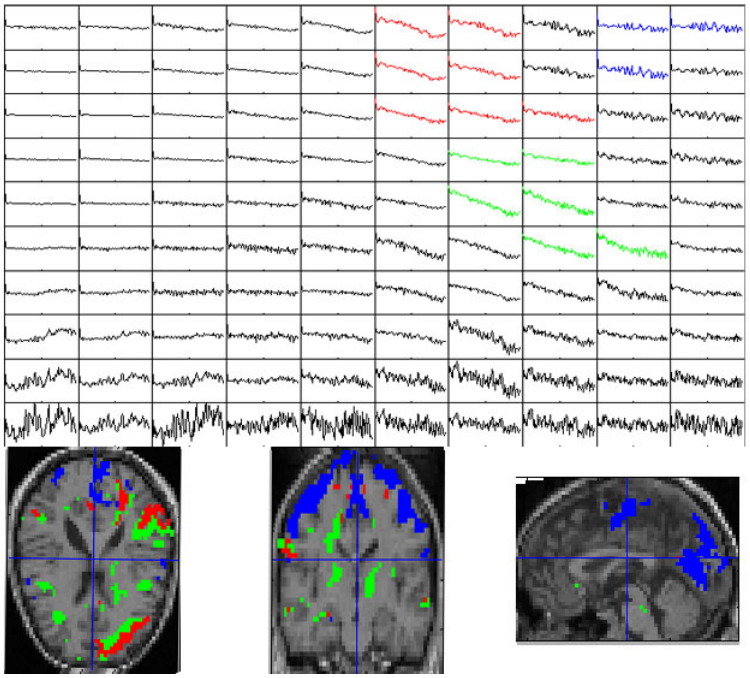

Figure 4.5: Projection of a set of clusters into the anatomical space of the brain.

The initialization of the arrays in the map can be done in numerous ways. Initializing the neurons with zero values or random noise is possible. One other way is to choose random TCs from the data to represent the initial values of the map. Other classical approach is also wildly used, and consists in the application of principal component analysis. In this case is possible to obtain the most significant Eigen vectors from the data, which represent the attribute combination most abundant in the data set. By selecting the TCs with minimal distance to these vectors it is possible to initialize the map with the TCs which better represent the variation of the data. The advantage of this method is that the algorithm will require lesser steps to achieve a stable state.

In many applications of the SOM is also common to observe some normalization of the data, but we will cover this aspect in more detail in the Implementation section.

4.2.2 Selecting a TC

There are two main ways the data can be "*fed*" into the map. In the first the training of the map is made iteratively by selecting a random TC from the measured data from the entire imaged volume or from a region of interest. In the second, all data is presented to the map in each iteration (this is normally called the batch version of the SOM). In both cases what defines the iteration are the parameters values. In the first case the parameters update after each random TC is presented to the map, in the second these values are only changed after the whole data is presented. The batch version is a good alternative when analyzing the whole brain as a means of assuring the whole set of TCs are presented to the map and the same number of times. Also in this version of the algorithm a fewer number of iterations are needed to reach the map convergence. When feeding a random TC to the map per iteration a common practice is to run the algorithm several times. Since in this case the maps delivered by the algorithm can greatly vary, running it several times allows the later selection of the best results.

4.2.3 Finding the winner

For each TC presented to the map the algorithm looks for the neuron that is more similar to the input and declares it the winner. The determination of the degree of similarity can be done using various methods and types of distance functions. Next we present two of these methods to determine similarity between vectors. The first uses the scalar product of the input and the tested neuron:

$$net_k = \sum_{j}^{N} [x_{ij} * n_{kj}] \tag{4.1}$$

where x_{ij} represents the jth component of the voxel i time-course and n_{kj} denotes the jth component of the neuron k. The scalar product represents the projection of one vector over another and is equal to the cosine of the angle between the unity vectors. This is one reason why the vectors are normalized. A scalar product with the result of 1 will mean that the vectors x_i and k_j are collinear and point in the same direction. As such they have similar parame-

ters. A zero value of the scalar product represents two perpendicular vectors and considerable differences in their parameters. One second possible way of determine similarity between the two vectors is the Euclidean distance:

$$net_k = \sqrt{\sum_{j}^{N} [x_{ij} - n_{kj}]^2} \tag{4.2}$$

A result of zero will mean that the two vectors are identical. These calculations will be performed for all the neurons in the map, and the one with highest value from the scalar product or lowest value from the Euclidean distance will be chosen.

4.2.4 Updating the neurons values and algorithm parameters

The winner cluster center found one the previous step will be moved towards the selected input as all the centers of the neighbor neurons by an amount inversely to the distance to the winner neuron using

$$n_k(t+1) = n_k(t) + h_{ck}(t) * (x_i(t) - n_k(t)) \tag{4.3}$$

where t is the current iteration value, h_{ck} is a neighborhood function that controls how much the winner and his neighbors are updated and to what degree, and x_i is the selected TC. As the algorithm goes on, the centers of the winning cluster and the considered current neighbors will change less, as a means of achieving the map convergence and preserving the quantization of the data. As the iterations progresses, the neighborhood function shrinks the neighborhood and at the end only individual nodes are updated. This function could be defined in numerous ways, being a shrinking Gaussian neighborhood function one of the most used (Kohonen, 1998):

$$h_{ck} = \alpha(t) * exp(-\frac{\|r_k - r_c\|^2}{2\sigma^2(t)}) \tag{4.4}$$

where $0 < \alpha(t) < 1$ is the learning rate, that decreases over time, controling how faster the neurons learn, and $r_k \in \Re^2$ and $r_c \in \Re^2$ are neuron coordinates from the winner and updated neuron respectively. Finally $\sigma(t)$ corresponds to

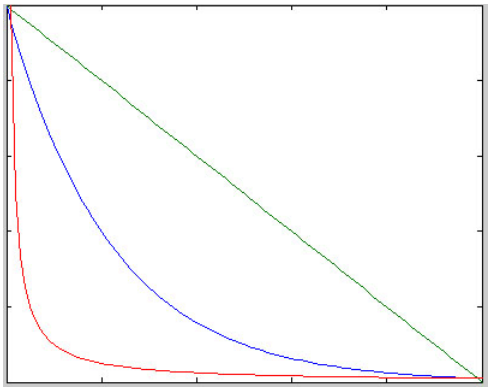

Figure 4.6: Example of SOM parameters updating functions: Linear (green), power-series (blue) and inverse-of-time (red).

the width of the neighborhood function, which also decreases with time. Many functions can be used to update the parameters. As an example we mention three of the most commonly used ones: linear, power-series and inverse-of-time functions (see Figure 4.6).

4.2.5 The end of the training process

The ending of the training processes could be based in a chosen number of iterations or on an evaluation of the quality of the obtained map. With map training we obtained a set of small clusters as large as the map's size. The clusters can then be combined to form larger super clusters. This can be done in a different number of ways. One approach would be to add small clusters interactively to the super clusters with the support of some visualization technique (Hkkinen and Koikkalainen, 1997). Other ways include automatic calculation of the super clusters by means of constraint (need-driven) clustering using metrics like least-mutual distance (Murtagh, 1995) or least-squares distance (Peltier et al., 2003), or can also be done using data-driven clustering like fuzzy c-means clustering (Chuang et al., 1999).

Chapter 5

Experimental evidence

Now that we established the principles behind the self organizing maps, we will try to gather evidence of the validity and interest of the method when analyzing fMRI experiments. Since this is a model free approach, it has the objective to find structure in the data without any knowledge about the experiment. With this assumption, it is difficult to conclude whether or not the results obtained are valid, or what is the significance of unknown areas of activation found in the brain by the method. This problem is even more complex since many of the mechanisms of the brain are a mystery and still being investigated by the research community. Since our objective is to prove the validity of the method, we will have to use it in experiments with known expected results. Our approach will be to analyze experiments that involve known functions and areas of the brain. Two of these areas are the visual and auditory cortex. More than this, we will test if our model free approach, without any needs for experimental information, is capable of delivering the same results of a hypothesis driven approach, in this case those that apply the General Linear Model like SPM.

For our study we implemented a package to analyze brain function using the self organizing maps algorithm. The package was then tested with data from an auditory and visual experiment. In this chapter we will talk about our implementation and methods, the results from our analysis and we will conclude with a discussion of these same results and the SOM approach.

5.1 Implementation and methods

Our analysis of the performance of the SOM algorithm will be based in two experiments, one based in the stimulation of the auditory cortex and other in the stimulation of the visual cortex.

The first data set obtained from the first experience comprises whole brain EPI-BOLD images acquired on a 2T Siemens MAGNETOM Vision system. 96 acquisitions were made with TR = 7s and each acquisition consisted of 64 contiguous slices (64x64x64 3mm x 3mm x 3mm voxels). This was a block design experiment where auditory stimulation was alternated with rest periods. The blocks of auditory stimulation consisted on bi-syllabic words presented to subject at a rate of 60 per minute. The experiment was conducted by Geraint Rees under the direction of Karl Friston and the FIL methods group. This experiment has not been formally written up and is freely available for education and evaluation purposes. The data set and a more detailed description can be found at `http://www.fil.ion.ucl.ac.uk/spm/data/auditory/`. The chapter 28 of the SPM5 manual (`http://www.fil.ion.ucl.ac.uk/spm/doc/spm5_manual.pdf`) illustrates a step by step analysis of this data set, using the SPM5 package, presenting the respective final results. We will compare these results to those obtained by our SOM approach using the same data set.

The second data set is composed of whole brain EPI-BOLD images acquired on a 3T Philips MRI system. 108 acquisitions were made with TR = 3s and each acquisition consisted of 40 contiguous slices (80x80x40 $\sim$ 2.875 x 2.875 mm x 3 mm voxels). This experiment used a rapid event-related paradigm design where various pairs of faces were presented in one of 6 possible orientations: 0, 60, 120, 180, 240 or 300. The above experiment was previously analyzed using hypothesis driven analysis by other investigation team (Saiote et al.) using FSL (fMRI software library - `www.fmrib.ox.ac.uk/fsl`) for the preprocessing and application of the GLM. In this particular experiment the investigation team tried to find not only activation in the visual cortex (Figure 4.12) but also more specialized zones (Figure 4.14) within this cortex related to the face inversion effect (FIE). Using the SOM approach we explored the data in order to find first one zone correspondent to the visual cortex activation and similar to the one found with the GLM approach. Later we also tried to find

within this same zone smaller specialized zones of activation.

In both analysis using the model driven approach, it was performed a single subject analysis in the first case and a multi-subject in the second case. We will compare our results with the results of these experiments, but using single subject analysis in both cases. In the second experiment we opted to choose a subject randomly instead of using the data from all of them.

To test the interest and validity of the SOM algorithm in fMRI analysis of the above described data sets and in general, we developed a software package using Matlab and the programming language C. The software offers the possibility to work with data with image (.img) format and NIfTI (.nii) format. A more detailed description of the application can be found in annex (see fSOM - user guide). For the two experiments the RAW data was preprocessed using the SPM5 package. In both cases the steps were the same:

1. Spatial preprocessing with realignment of the fMRI images.
2. Coregistration between structural and functional data.
3. Normalization of the data onto a standard anatomical template.
4. Smoothing of the data using a Gaussian smoothing kernel of 8.

In both cases each time course was subtracted by its mean. In the fMRI images the signal correspondent to the BOLD response is very low compared to the structural signal. If this "*normalization*" of the data is not done, the SOM algorithm will organize the data based on the structural component of the data. One example of the algorithm partitioning without the initial subtraction of the mean is shown in Figure 5.1. As we can see the algorithm found clusters representing different parts of the structure of the brain, in this case white matter, instead of founding clusters that represent brain function. This step of subtracting the mean to the time-courses is done automatically by our application and has the objective of normalize the data to account only for its variance, and to avoid convergence of the SOM algorithm based on the mean values of the time courses. Other step taken before running the algorithm was the application of a threshold to both data sets, as a means of excluding from the analysis voxels outside of the brain structure.

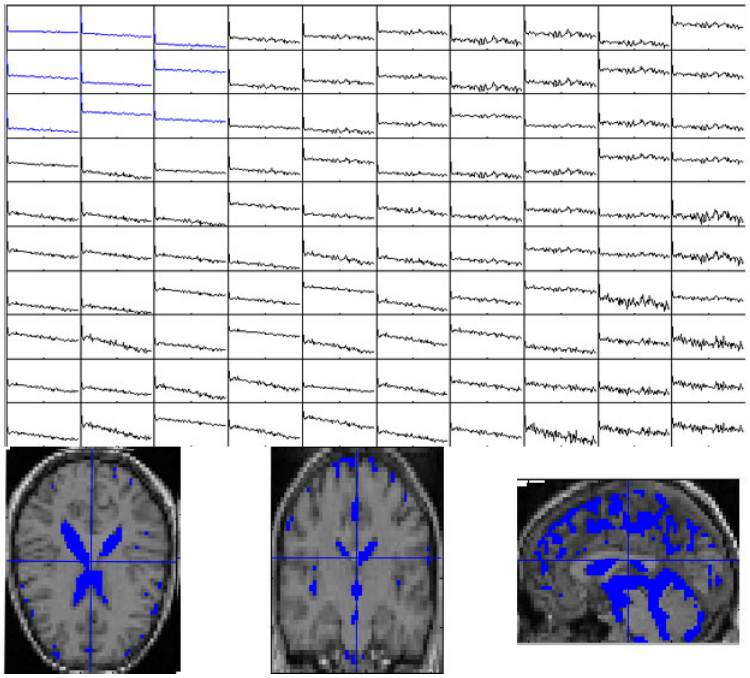

Figure 5.1: Clusters found by the SOM algorithm mapping brain structure rather than brain function.

After the steps taken above we applied our algorithm. The metric used to the determination of the degree of similarity between the time courses was the Euclidean distance. The chosen neighborhood function was a Gaussian neighborhood function as it was defined in Equation 4.4. A quadratic grid of 10 x 10 was used throughout both experiments giving a total of 100 nodes per map, each node representing a mean of about 40-50 TCs. The choice of 100 exemplar time courses represented by each node, in general, seems an ample enough size to classify 5 to 6 possible fMRI cluster types (activation, head motion, functional connectivity, and noise, among other possibilities). The SOM map was initialized with random noise. At each iteration of the algorithm all time courses of interest were presented to the map. The training of the neuron map was made in a two stage process. In the first stage the number of iterations was set to 10, which represents that the whole data was processed 10 times by the algorithm. The initial Gaussian smooth kernel was set to 6 and the initial learning rate to 0.05. In the second phase, called

calibration, the total number of iterations was set to 100, the initial Gaussian smooth kernel to 3 and the initial learning rate to 0.001. For the updating of the training parameters (Gaussian smooth kernel and learning rate) was used a power series function (Figure 4.6).

In the case of the first experiment the results werent total satisfactory, and so a second analysis was made. In this second approach we selected a smaller ROI to be analyzed by the algorithm. Only voxels from the slices that were known to contain the known activation area (auditory cortex) were presented to the SOM, rather than the whole brain. As we will see the definition of a smaller ROI will represent much more conclusive results.

The largest data set analyzed was composed by 108 frames and a ROI of 52779 voxels. In this case it took about 7 minutes to train the map on a virtual machine with an equivalent processor of 2.2 GHz and 1024 MB of RAM.

The final results were analyzed with the support of a homemade visual tool. By trial and error we tried to merge the map nodes into superclusters until we obtained areas of activation similar to those that were expected from the experiments. Nodes that represented scattered voxels in brain were considered some kind of noise and were discarded as a contribution to an activation of interest. Besides trying to identify previously known regions of activation, found in the hypothesis driven experiences, we also tried to explore the capabilities of the SOM in finding other zones of activation related to the experiment. Although we dont have the expertise or the knowledge to interpret these results, this action has the objective to empathize the SOM capability in discovering non-expected behaviors from the brain that maybe would be worth exploring.

5.2 Results

For each experiment a self organizing map of 10 x 10 with 100 nodes was obtained. Like we already mentioned, this map was explored using a visualization tool with the objective of finding zones of activation similar to those found by hypothesis driven analysis. In this subsection we will show our results and well make the respective comparison between the SOM approach and the other inferential data analysis paradigms results.

5.2.1 Experiment 1: auditory fMRI data

First we present the results achieved with SPM by applying a t-contrast, with a $p = 0.05$. Using an adequate design matrix the results obtained are shown in Figure 5.2. Analysis of the data was also made using our SOM algorithm. First we trained the map using the time courses from all brain and found similar areas of activation in the auditory cortex by defining a supercluster composed by 4 nodes (Figure 5.3). Although auditory cortex regions were found by our algorithm, we can see that other areas outside this cortex are also activated. It is possible that this other regions can have a relation to the experiment and the auditory stimulus, since they are strongly correlated. Nevertheless one of our objectives was to demonstrate that our algorithm could deliver similar results to the hypothesis driven ones. To see if we could obtain better results, more like the ones delivered from SPM, we trained another map. This time we only used a data set composed from the slices of the brain we knew that contained the wanted areas of activation, the slices where the auditory cortex is located. Defining a supercluster of 2 nodes we achieved more satisfactory results as we can see in Figure 5.4 and by comparing with Figure 5.2.

In a second phase of analysis of the trained map we tried to find other unknown homogenous zones of activation as a means of exploring unknown brain behavior. This is a great example of how the SOM can be used we analyzing brain function. We found one other interesting zone represented by 5 nodes of the map (Figure 5.5). Although we do not have sufficient knowledge to interpret this result, we know for a fact that the found homogeneous area represents a certain behavior of the brain during the experiment. The data driven approaches represent methods that find structure in the data, but they do not give us a meaning to the divisions made. As we will discuss later, the SOM is a good way to explore the function of the brain when information of the experiment is not available or when we have complex experiments difficult to model. Because of this the SOM, like other data driven approaches must be most of the times complemented with model driven methods and the expertise of the researchers, so that can be given meaning to the division of the data.

5.2.2 Experiment 2: visual fMRI data

The results with a GLM approach using FSL are shown in Figure 5.6. The areas of activation are a result of a multi-subject analysis and our analysis was done using data from only one subject chosen randomly. Knowing this, it is reasonable to assume that our results can not be a perfect match to those shown before. In Figure 5.7 we see the areas of activation found using our SOM analysis algorithm. By grouping 15 nodes into a supercluester we can see activations, in the zone of the visual cortex, similar to the ones obtained using FSL and multi-subject analysis.

Also with the GLM approach there were in a second phase identified five functional ROI in the subjects (Figure 5.8). These areas are identified in the figure by three different color clusters. We tried to explore the capabilities of the SOM in finding similar areas and smaller clusters within the data set. For this, we tried to divide our 15 nodes supercluester in a set of three smaller superclusters. As we can see in Figure 5.9, we found three homogeneous and symmetric areas of activation with this division. Because we do not have the expertise and we are using a model free approach without any information about the experiment, we cannot give a meaningful interpretation to this division. Nevertheless we know that this found ROIs represent different behaviors, and from this we can propose an hypothesis stating that these areas perform different functions within the visual cortex. Also if we compare the three smaller clusters obtained, we can see some similarities to the zones found by the GLM approach in figure 5.8.

5.3 Discussion

The self organizing map (SOM) approach was applied to two experiments. These experiments were previously analyzed by other investigating teams using model driven approaches based on the general linear model (GLM). The GLM method requires knowledge about the experiment and involves the construction of a model function that describes the experimental protocol. Our SOM approach did not require any external reference. Model free methods offer a great alternative to fMRI analysis by analyzing the data based on sig-

nal alone without user bias. This is a very important characteristic in cases where we have complex experimental protocols or when we are dealing with unknown response functions that hardly can be model correctly by the user (e.g. memory studies). Nevertheless, model free approaches only find structure in the data without giving this structure any meaning. The researchers expertise is needed to interpret the results and these methods may have to be complemented with inferential analysis as a means of associating the partitioning of the data to the experimental protocol. In our analysis we did not have exactly the expertise to interpret the structuring of the data made by the SOM algorithm. In our case, we used the portioning of the data delivered by the SOM and tried to isolate homogeneous zones of activation in the brain that were similar to those found in other approaches and that were located in the known cortexes related to the experiment. The results were within our expectations. With our SOM algorithm we achieved similar results to those found with the model driven methods, finding zones of activation in the brain within the expected cortexes (the auditory in the first experiment and the visual in the second experiment).

More than to find similar zones of activation we also tried to find homogeneous zones not represented in the results delivered by the GLM approach and outside the cortexes supposedly involved in the experiments. We did this regarding the auditory experiment and found a zone of interest outside the auditory cortex that could be somewhat related to the experimental protocol (Figure 5.5). Although this is not conclusive, this example has the objective of strengthening the capabilities of the SOM in finding unexpected responses of the brain and its capabilities as a research tool.

The SOM method also offers a good alternative to other data driven approaches. It does not have to deal with the constraints of orthogonality and independency of the data of the PCA and ICA approaches respectively and addresses some of the difficulties of other clustering algorithms as we already mentioned previously. K-Means clustering (KMC) for example would be able to find differently sized and populated clusters. Unfortunately this property cannot be assumed in the case of fMRI analysis, since the clusters in the data are severely blurred and have high mutual proximity. This problem of the KMC is even worst when we normalize the data to make clustering more sensitive

to the dynamics of the brain rather than the time-courses mean values. KMC can still do well when separating noise from the signal of interest. However if we set the algorithm to find a small number of clusters it would miss small zones of activation. These zones would simply be grouped into a single larger cluster. KMC by minimizing the sum of squared distances has the tendency to equalize the sizes of identified clusters which difficult the detection of small and larger clusters within the same data set. This can be solved by setting a large number of initial clusters. Although this makes possible to find smaller zones of activation, this zones will be represented by different independent clusters. A way to solve this is to merge these small clusters that are supposed to belong together. In the other hand if we have a larger cluster representative of a larger zone of activation and we want to divide it in smaller specialized zones the solution would be to partition it into smaller clusters. Both options are supported by the SOM approach. This was done in experiment 2 by dividing the larger cluster (Figure 5.7) into a set of 3 smaller clusters (Figure 5.9). With this operation it was possible to find more specialized zones with different behaviors within the visual cortex. This characteristic of the SOM also deals with the problem of the validity of the portioning of the KMC. By merging nodes interactively it is possible to define which nodes should belong together within the same cluster and which nodes do not contribute to activations of interest.

Regarding the SOM algorithm alone it is visible that the results depend on a number of factors and variables:

- The method of initialization of the map.
- The number of iterations and the size of the map.
- The learning rate and the neighborhood width variables.
- The distance metric.
- Functions that define the updating of the variables and the neighborhood function.
- The method to form superclusters.

All this factors strengthen the idea that running the algorithm with alternative functions and values might be a good idea in order to find the best results. These variables can all be chosen using common sense, by experimenting or with the help of common practice references.

Automatisms can also be used to optimize the algorithm or to reduce user bias. For example a mean squared error (MSQE) (Peltier et al., 2003) between time courses can be calculated at each iteration of the algorithm to access about its convergence. With this mechanism it is possible to stop the algorithm at an iteration where no further appreciable changes in the map occur. The calculation of supercluesters can also be made automatically with the support of methods like contiguity constraint clustering (Fischer and Hennig, 1999) which merges neighboring nodes with least mutual distances. Although the automatic formation of superclusters seems to be a good method to reduce the user bias, we cannot underestimate the power of an interactive method (our approach) based on the researchers expertise and the visual capabilities offered by the SOMs topographical mapping of high-dimensional data.

The SOM learning rate or neighborhood contraction rate can also be optimized by finding which values attain the lowest total squared error (Peltier et al., 2003) for example. This represents a great alternative when choosing the best values to these variables.

As we also have observed the choosing of smaller ROIs can help to improve the results returned by the SOM, as we eliminate form the training process the contributions of less interesting time courses. Although normally a 10x10 grid of 100 nodes seems to be sufficient to characterize different types of signals, a larger grid can sometimes be a better option to find even smaller and specialized zones of activation.

Extracting extra properties from the maps delivered by the SOM can also help to better characterize the data. Gradient images that calculate the averaged distance between neighborhood nodes and frequency plots that count the number of time-courses for each node can help in defining how many clusters distinct clusters exist in the data. Also calculating the average spatial distance between the nodes in the map could make easier to detect which nodes in the feature space form clusters in the image pane.

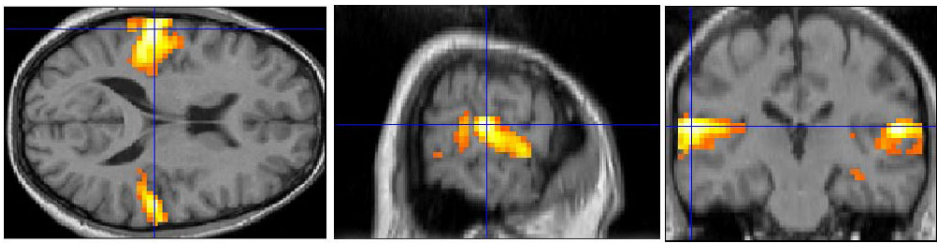

Figure 5.2: Areas of activation obtained from auditory data of whole brain running SPM.

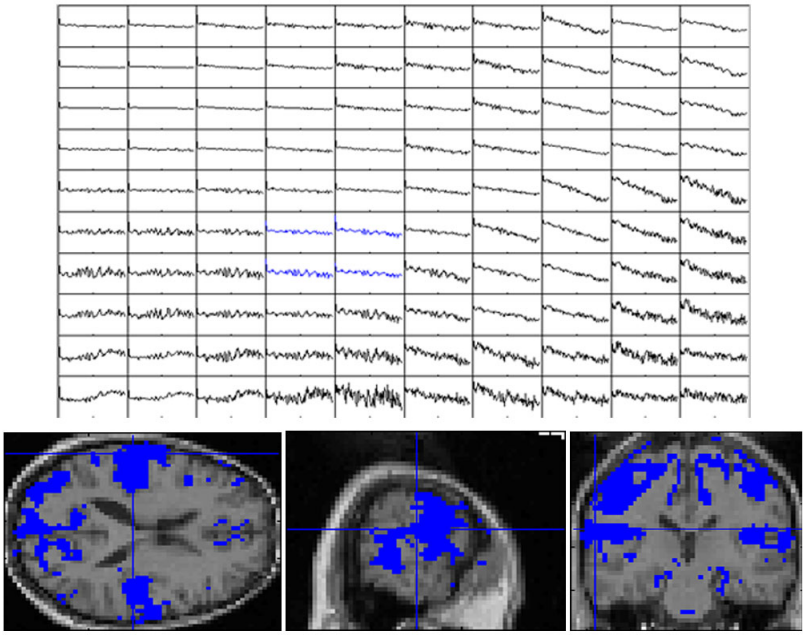

Figure 5.3: Areas of activation obtained from auditory experiment data of whole brain running our SOM algorithm.

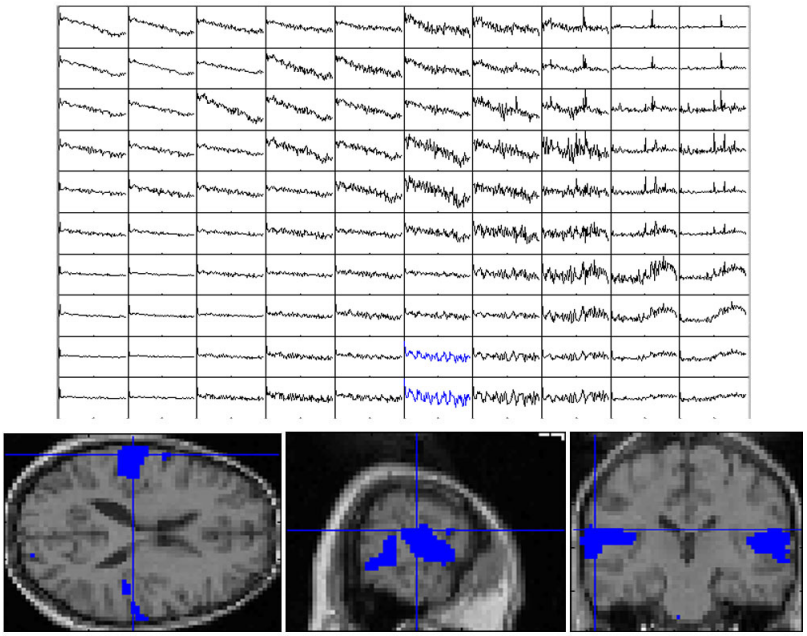

Figure 5.4: Areas of activation obtained from auditory experiment data (only from slices which were known to contain the expected responses) running our SOM algorithm.

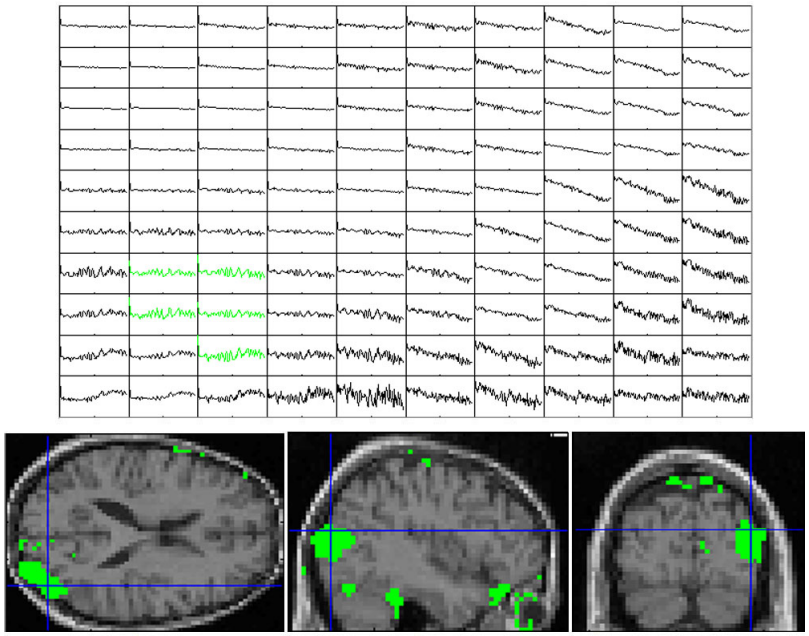

Figure 5.5: Unknown areas of activation obtained from auditory experiment data running our SOM algorithm.

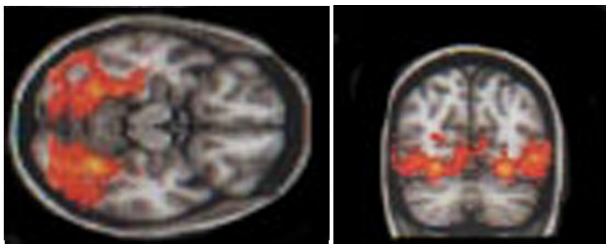

Figure 5.6: Group activation maps obtained from visual experiment data ($p < 0.05$) using a GLM approach (Saiote et al.).

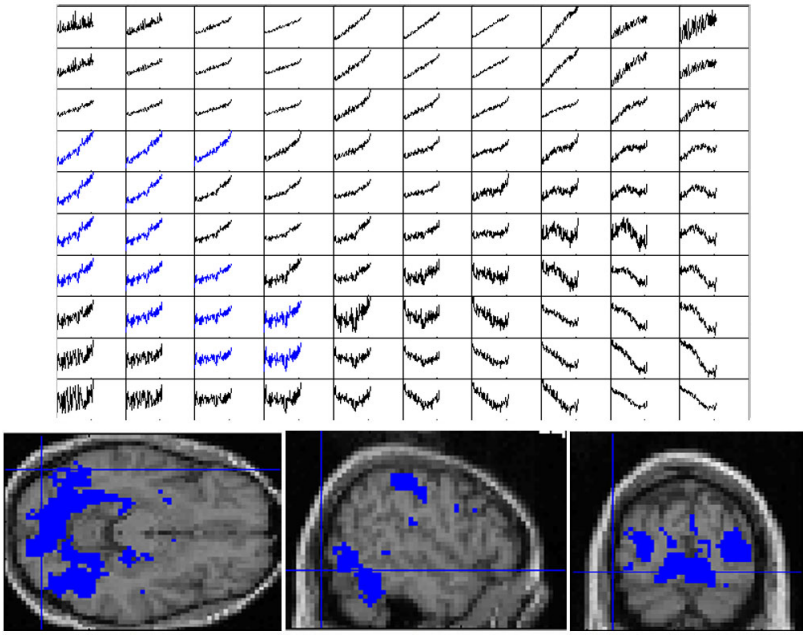

Figure 5.7: ROI obtained within visual cortex from visual experiment data of whole brain running our SOM algorithm. The results are very similar to those delivered by the GLM approach (Figure 5.6). Although they are not exactly the same, we must not forget that the results from GLM derive from a multi-subject analysis and these ones from a single-subject approach.

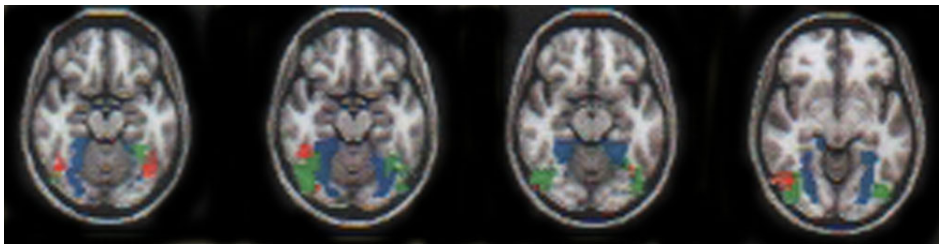

Figure 5.8: Example of five functional ROIs identified in the subjecs: FFA (fusiform face area) and OFG (occiptal fusiform gyrus) in blue, PPA (parahippocampal place area) in red and LOC (lateral occiptal cortex) and MFO (middle fusiform object are) in green (Saiote et al.).

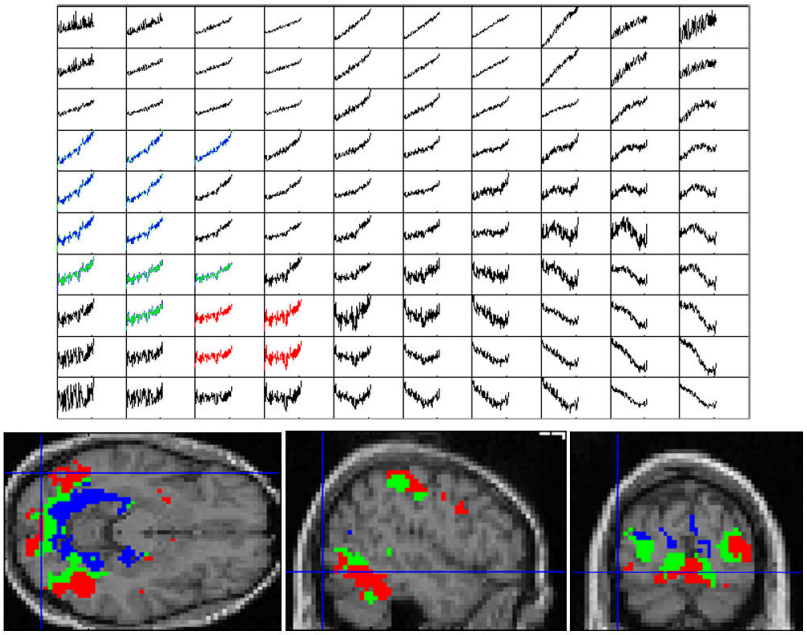

Figure 5.9: Smaller areas of activation within the visual cortex obtained by dividing the initial supercluester into smaller supercluster with SOM approach. With our division we tried to obtain a similar partitioning to that obtained with the GLM approach. As we can see, although the areas obtained running SOM are larger to those delivered with the GLM method, we identified three ROIs within, more or less, the same space of the ROIs identified in figure 5.8 (GLM approach).

Chapter 6

Conclusion

Through this thesis, we hopefully provided an illustrative overview of the fMRI technique, including the physical principles, the elements of an fMRI experiment and analysis approaches.

Regarding the focus or our work study, the analysis techniques, we have to mention that during our research we came across not only the techniques described here, but many others. Even the techniques described have many variants in many studies or are used in hybrid approaches with other ones. This leaves us to conclude about the complexity of the BOLD fMRI signal and the difficulty to obtain precise answers or to find a completely adequate analysis technique.

On the matter of model driven vs data driven approaches we conclude that both of them respond to different needs and must be seen as complementary. If in one side model driven techniques, like SPM, offer a great method to associate an experimental protocol to activation within the brain, data driven ones enable the structuring of the underlying brain signals without a priori knowledge. This characteristic of data driven methods is very important when we have complex experimental protocols and when we are dealing with unknown response functions. Nevertheless many investigators see the combination of these two approaches as the future o fMRI: ""*As the field continues to mature, We foresee the development of hybrid methods that will attempt to take advantage of these two complementary approaches: first employing powerful data-driven techniques to characterize the underlying nature of the signals*

and noise, then testing hypotheses of interest in the context of this accurate characterization" (Friston, 1998).

Regarding the data driven techniques we detailed some of the most used ones in the fMRI analysis. All of them offer an interesting approach to this subject and are detailed in many studies with interesting results. When choosing which technique to apply we must consider strengths and limitations inherent to each one. Methods like ICA and PCM separate the fMRI BOLD signal into several well defined components but have to deal with constraints of independency and orthogonality of these components. Advanced cluster algorithms can be very useful in finding differently activated pattern resulting from complex simulation or high temporal resolution, but have also their problems to address: the validity of clusters, the choosing of number of expected clusters and the problem in finding clusters with different dimensions.

In this thesis we tried to conclude about the interest of the SOM algorithm when analyzing fMRI experiments. We analyzed two data sets from two different experiments, without any external knowledge about the experiment, and achieved satisfactory results. Not only we found activation within the expected cortexes of the brain but also obtained results very similar to the ones found in previous studies with a general linear model approach. We also tried to find other zones of activation not present in the previous studies. For this we used visualization techniques and a trial and error method. We assumed that homogeneous zones of activation found within the brain represented some kind of interesting activation and should not be considered noise. Although we do not have the expertise or the knowledge to interpret our findings, we did this to strengthen the fact that the SOM approach can be a powerful investigating tool when analyzing unknown responses. Finally we tried to demonstrate the capacity of SOM in overcoming some of the typical clustering algorithms limitations.

During our research and experiments SOM proved to be a very flexible approach that, as we have discussed, addresses the typical clustering problems while maintaining the advantages of this kind of approach. It also can be used as a method of initialization to other algorithms as the fuzzy C-means clustering. The algorithm topological ordering with the help of visualization techniques proved to be a great means to visualize complex data and to in-

vestigate the overall dynamics of an experiment. On the downside the SOM approach is dependent of many factors, like initialization, parameters definition and others. Although this is true, we discussed a number of methods that can be used to introduce more automatisms into the algorithm and reduce the user bias.

In our work we tried to illustrate how SOM can be used to analyze fMRI data and some of the results obtained with this approach. We cannot answer with our study the question of statistical significance but we tried to discuss and show why the SOM approach can be interesting in terms of fMRI analysis. With this idea in mind, we hope this thesis encourages further research in this matter with the achievement of promising results, bringing us one step closer to understand more clearly how our brain works.

Appendices

Appendix A - fSOM: user guide

fSOM is a tool developed to analyze fMRI data using the self-organizing maps approach. The tool was developed using the programming language C for running the algorithm and Matlab for user interface and data manipulation. The use of this software package requires the previous installation of SPM5. fSOM supports image (.img) and NIFTI (.nii) formats. The software tool does not implement any preprocessing steps, so all preprocessing must be done using other tools like SPM. fSOM is divided in two smaller applications, one for training of fMRI data (fSOMT) and other for anatomical mapping (fSOMM) of the results obtained from data training. Our application will be integrated into a well established fMRI data analysis software package (`SPM-http://www.fil.ion.ucl.ac.uk/spm/`) and will be made publicly available. We will next present a very simplistic user guide for both applications.

fSOMT: Data Training

To run fSOMT first we must type 'fSOMT' in the Matlab work space. For this we have to be either on the package folder (fSOM) or we must add the correspondent path. After we initiate the application we will have a window like in Figure 6.1.

The first step is to load the data with the 'Load Data' button. After this a panel with information about the data is shown (see Figure 6.2). This panel contains information about the dimensionality of the data, the total number of voxels present in the data set and the ones considered in the training process

when a certain threshold is applied.

The next step consists in applying a threshold value in order to eliminate from training voxels outside the brain region. Initially the value of the threshold is zero and because of that the info panel indicates that the number of 'Analyzed voxels' is the same as the 'Total number of voxels'. Filling the field Threshold and pushing the button 'See' enables the user to observe which areas of the image are being used for the training process (Figure 6.3). When an adequate value is found pushing the 'Apply' button will submit the new interest area and update the value 'Analyzed voxels' in the info panel correspondent to the voxels considered for the training process.

After the threshold is applied we can start to choose the algorithm running options and fill the parameters. First we set the type of initialization. For default the nodes on the map are initialized with zero values. By setting the first options these nodes will be initialized with values ranged from the minimum to maximum value present on the data set. The second option enables the initial map to contain the values from a previous trained and saved map. This feature is used for the calibration process.

Next we choose the algorithm type. Standard mode will pick a random time course from the data at each iteration to be presented to the map. All data mode will present all time courses at each iteration. After choosing the algorithm type we must choose the type of functions that will be used to update the training parameters. There are two options in this case, 'Linear and 'Power series function.

The final step consists in setting the SOM parameters values: number of iterations of the algorithm; initial and final learning rate; initial and final neighborhood width; and some size (map width and height). After all desired options are chosen and the parameter values are set, pressing the 'Train button will start the training process.

fSOMM: Mapping results into the brain anatomical space

To run fSOMM first we must type 'fSOMM' in the Matlab work space. For this we have to be either on the package folder (fSOM) or we must add the correspondent path. After we initiate the application we will have a window

like in Figure 6.6.

The first steps in order consist in loading the data used in the training process, load an image for co-registration and load the map obtained in training phase. For this we use the buttons ‘Load Data, ‘Load Correg and ‘Open Map respectively.

After these steps, the map obtained in the training phase will be shown in the SOM panel (Figure 6.7). By setting values ranged from zero to one on the RGB value boxes, it is possible to define the colors we want to apply to each map node. Left clicking in the node zone will change its color to the one defined by the RGB values and the enables the user to define different super clusters. An example of a definition of two superclusters is shown also in Figure 6.7, where we see one of the supercluster composed by nodes in red and the other by yellow nodes.

The final step consists in pushing the ‘Map button. By pushing this button, the application will open a new window with a representation of the brain, where the voxels will have the same color of the node which have the most similar behavior to their time courses (Figure 6.8). In this case the used metric is the Euclidean Distance, the same metric used in the training process. The voxels represented by nodes with a black color (RGB = (0,0,0)) will maintain the same color they had in the anatomical image loaded by the co-registration step. The Slice Viewer, represented in Figure 6.8, enables the user to navigate through the slices by clicking in zones of the image. It is also possible to have multiple slice viewer windows opened in order to compare different supercluster.

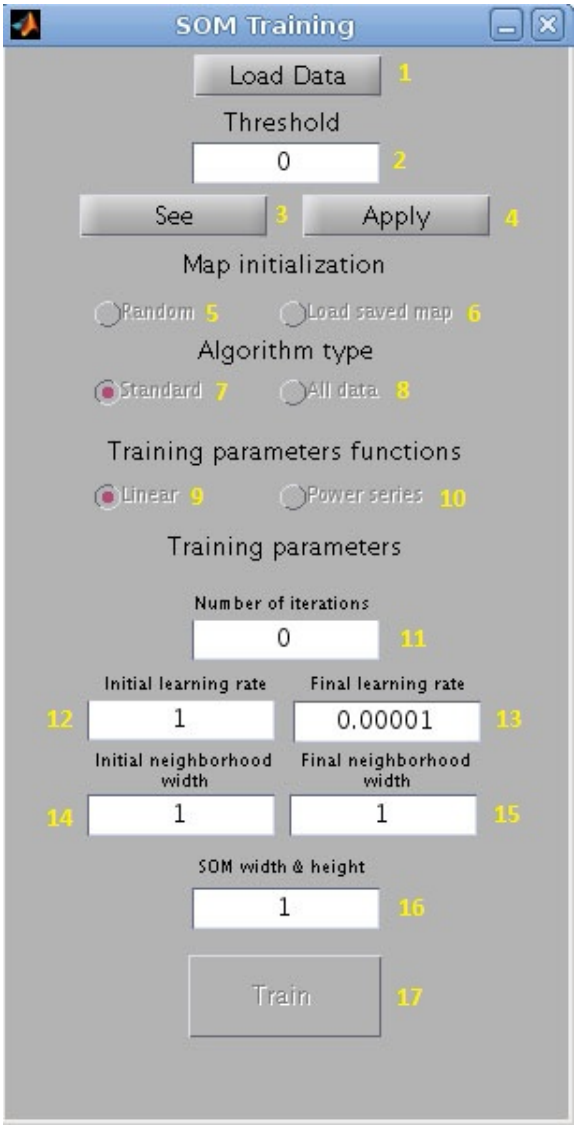

Figure 6.1: fSOMT interface: **1-**Load data button; **2-**Box where image threshold is defined; **3-**Button to see image with applied threshold in 2; **4-**Button to apply defined threshold to data; **5-**Random initialization of the map; **6-**Initialization based on a previously saved map; **7-**Standard algorithm processing (one time-course per iteration); **8-**All data algorithm processing (all time-courses per iteration); **9-**Linear evolution of the training parameters;**10-**Evolution of the training parameters using a power series function; **11-**Number of iterations of the algorithm; **12-**Initial learning rate; **13-**Final learning rate; **14-**Initial neighborhood width; **15-**Final neighborhood width; **16-**Size of the trained map (width and height); **17-**Button to initialize training process.

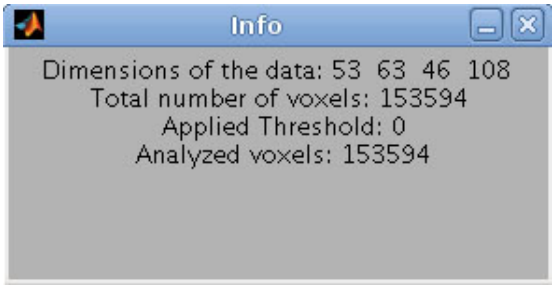

Figure 6.2: fSOMT info panel. As we can see the info panel shows information about the dimensionality of the data in the first line. The three first values correspond to the spacial coordinates (x,y and z) and the last to the temporal dimension. The second line defines the total number of voxels present in the data and the third the current applied threshold. Finally the fourth line represents the number of voxels considered on the training process after the application of threshold defined in line three.

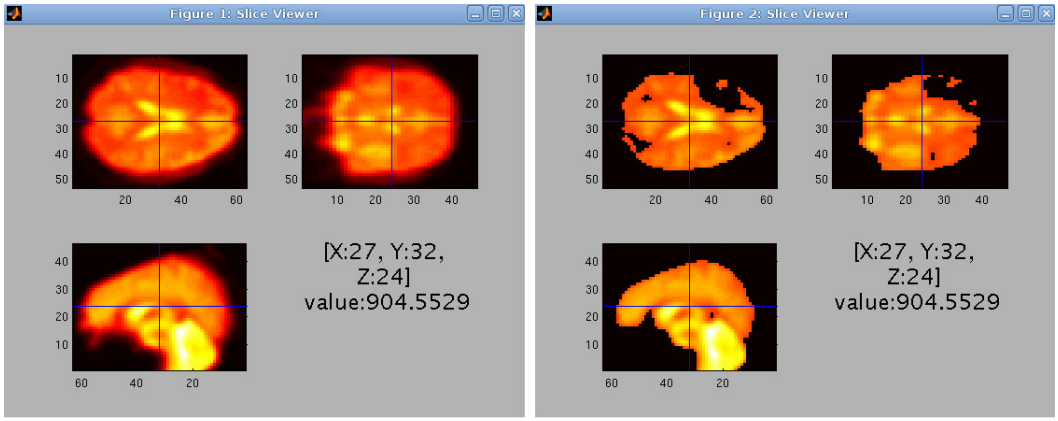

Figure 6.3: Different thresholds applied to an fMRI data set. In the first figure we see an image where there is no threshold applied (zero value). In the second it was applied a threshold of 700 and as a result only the colored zones with values above 700 are shown in the image.

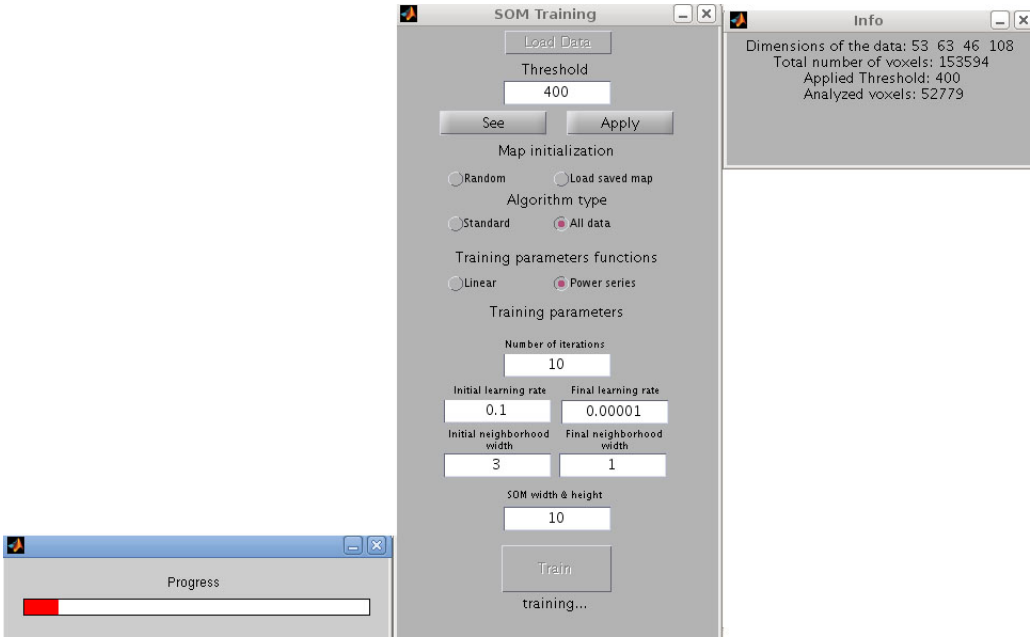

Figure 6.4: fSOMT interface with info panel and progress bar

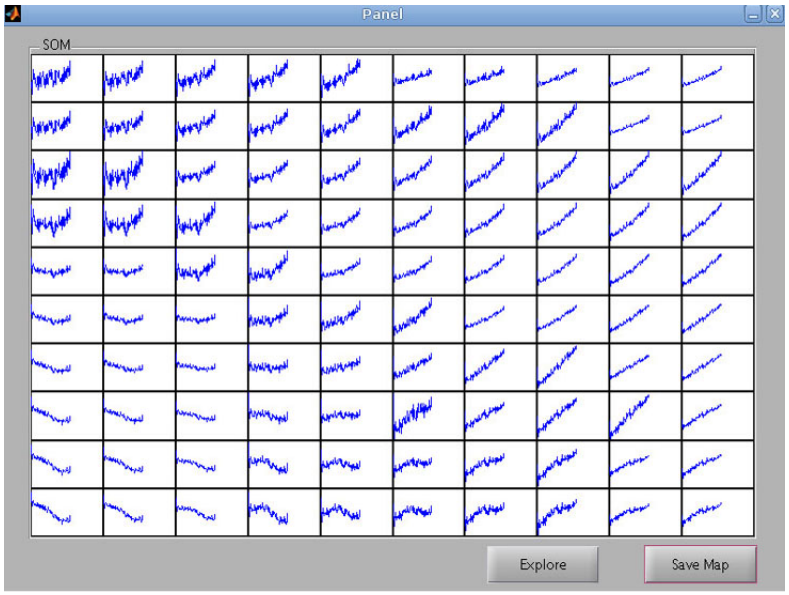

Figure 6.5: fSOMT results panel. The new panel shows the obtained map from training process. It is possible to further analyze the map in more detail or save it.

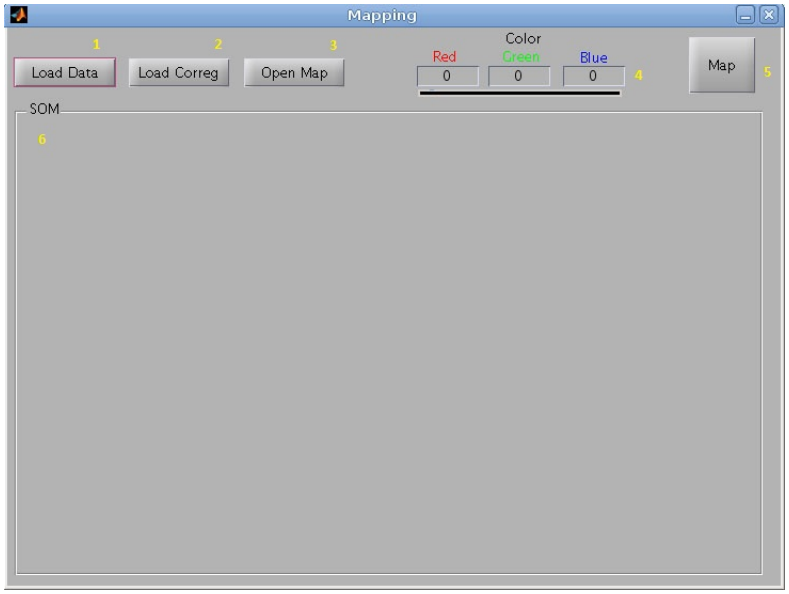

Figure 6.6: fSOMM interface: **1-**Load data button; **2-**Load Correg button; **3-**Load map button; **4-**RGB value boxes; **5-**Map button; **6-**SOM panel.

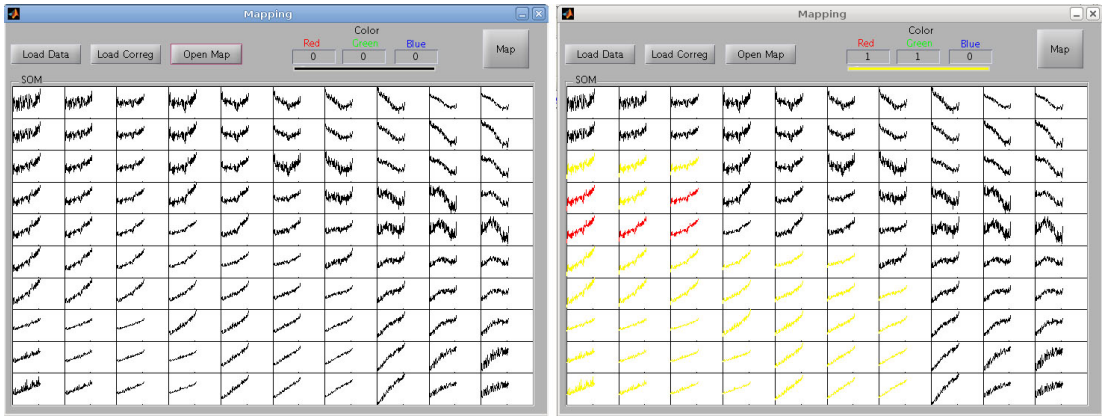

Figure 6.7: fSOMM interfaces with loaded map. In the first image we can see the fSOMM interface with the representation of the loaded map. In the second image we see the definition of two superclusters on the map by coloring a group of nodes with red and the other with yellow.

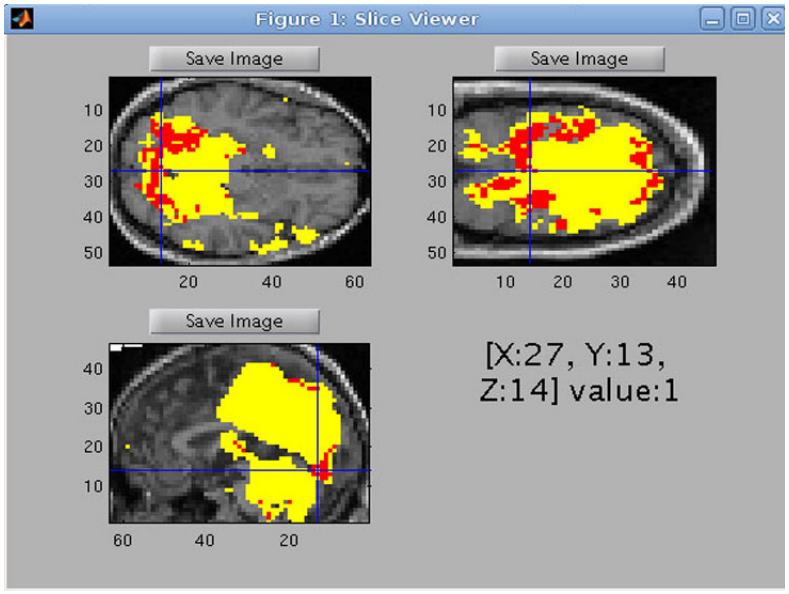

Figure 6.8: Slice Viewer with zones of activation. The voxels represented by the nodes colored in Figure 6.7 are represented in an anatomical image with the same color of each node.

Bibliography

A. Aersten and H. Preissl. *Non Linear Dynamics and Neuronal Networks*, chapter Dynamics of activity and connectivity in physiological neuronal networks, pages 281–302. VCH Publishers Inc., 1991.

Edson. Amaro Jr and Gareth J. Barker. Study design in fmri: Basic principles. *Brain and Cognition*, 60:220–232, 2006.

Anders H. Andersen, Don M. Gash, and Malcom J. Avison. Principal component analysis of the dynamic response measured by fmri: a generalized linear systems framework. *Magnetic Resonance Imaging*, 17:795–815, 1999.

R Baumgartner, L Ryner, W Richter, R Summers, M Jarmasz, and R Somorjai. Comparison of two exploratory data analysis methods for fmri: fuzzy clustering vs. principal component analysis. *Magnetic Resonance Imaging*, 18:89–94, 2000.

Richard Baumgartner, Gordon Scarth, Claudia Teichtmeister, Ray Somorjai, and Ewald Moser. Fuzzy clustering of gradient-echo functional mri in the human visual cortex. part i: Reproducibility. *Journal of Magnetic Resonance Imaging*, 7:1094 – 1101, 1997.

J. W. Belliveau, Kennedy D. N., R. C. McKinstry, B. R. Buchbinder, R. M. Weisskoff, M. S. Cohen, J. M. Vevea, T. J. Brady, and B. R. Rosen. Functional mapping of the human visual cortex by magnetic resonance imaging. *Science*, 254(November 1):716–719, 1991.

John W. Belliveau, Bruce R. Rosen, Howard L. Kantor, Richard R. Rzedzian, David N. Kennedy, Robert C. McKinstry, James M. Vevea, Mark S. Cohen, Ian L. Pykett, and Thomas J. Brady. Functional cerebral imaging by

susceptibility-contrast nmr. *Magnetic Resonance in Medicine*, 14:538–546, 1990.

BB Biswal and JL. Ulmer. Blind source separation of multiple signal sources of fmri data sets using independent component analysis. *J Comput Assist Tomogr.*, 23:265–271, 1999.

F Bloch. Nuclear induction. *Phys. Rev.*, 70:460–474, 1946.

M.J. Brammer. Head motion and its correction, volume functional mri. In *An Introduction to Methods*. Oxford: Oxford University Press, 2001.

Gyorgy Buzsaki, Kai Kaila, and Marcus Raichle. Inhibition and brain work. *Neuron*, 56(5):771–783, December 2007. doi: 10.1016/j.neuron.2007.11.008. URL `http://dx.doi.org/10.1016/j.neuron.2007.11.008`.

VD Calhoun, T. Adali, GD Pearlson, and JJ. Pekar. Spatial and temporal independent component analysis of functional mri data containing a pair of task-related waveforms. *Hum Brain Mapping*, 1:43–54, 2001.

Kai-Hsiang Chuang, Ming-Jang Chiu, Chung-Chih Lin, and Jyh-Horng Chen. Model free functional mri analysis using kohonen clustering neural network and fuzzy c-means. *IEEE Transactions on Medical Imaging*, 18:1117–1128, 1999.

M. DEsposito, E. Zarahn, and G. K. & Aguirre. Event-related functional mri: Implications for cognitive psychology. *Psychological Bulletin*, 125:155–164, 1999.

K. I. Diamantaras and S. Y. Kung. *Principal Component Neural Networks: Theory and Applications*. Wiley-Interscience, 1996.

X. Ding, J. Tkach, P. Ruggieri, and T. Masaryk. *Proceedings of the Society of Magnetic Resonance, Second Meeting, August 6–12, 1994, San Francisco, California*, chapter Analysis of the time-course functional data with clustering method without use of reference signal, page 630. Society of Magnetic Resonance, 1994.

X. Ding, T. Masaryk, P. Ruggieri, and J. Tkach. Detection of activation patterns in dynamic functional mri with a clustering technique. In *Proceedings of the International Society for Magnetic Resonance in Medicine, Fourth Scientific Meeting and Exhibition, Ney York, New York, USA, April 27 - May 3, 1996*, 1996.

Jeng-Ren Duannb, Tzyy-Ping Jungb, Wen-Jui Kuoc, Tzu-Chen Yehd, Scott Makeigb, Jen-Chuen Hsiehd, and Terrence J. Sejnowskib. Single-trial variability in event-related bold signals. *NeuroImage*, 15:823–835, 2000.

Peter Filzmoser, Richard Baumgartner, and Ewald Moser. A hierarchical clustering method for analyzing functional mr images. *Magnetic Resonance Imaging*, 17:817–826, 1999.

H. Fischer and J. Hennig. Neural network-based analysis of mr time series. *Magn Reson Med*, 41(1):124–131, January 1999. ISSN 0740-3194. URL `http://view.ncbi.nlm.nih.gov/pubmed/10025619`.

Jens Frahm, Klaus-Dietmar Merboldt, Wolfgang Hnicke, Andreas Kleinschmidt, and Henning Boecker. Brain or veinoxygenation or flow? on signal physiology in functional mri of human brain activation. *NMR in Biomedicine*, 7:45–53, 1994.

K. J. Friston, C. D. Frith, P. F. Liddle, and R. S. Frackowiak. Functional connectivity: the principal-component analysis of large (pet) data sets. *J Cereb Blood Flow Metab*, 13(1):5–14, January 1993. ISSN 0271-678X. URL `http://view.ncbi.nlm.nih.gov/pubmed/8417010`.

K. J. Friston, A. P. Holmes, K. J. Worsley, J.-P. Poline, C. D. Frith, and R. S. J. Frackowiak. Statistical parametric maps in functional imaging: A general linear approach. *Human Brain Mapping*, 2:189–210, 1995.

Karl J. Friston. Imaging cognitive anatomy. *Trends in Cognitive Sciences*, 1: 21–27, 1997a.

Karl J. Friston. Modes or models: a critique on independent component analysis for fmri. *Trends in Cognitive Sciences*, 2:373–375, 1998.

K.J. Friston. *Human Brain Function*, chapter Analysing brain images: principles and overview, pages 25–42. Academic Press USA, 1997b.

Alexander Geissler, Rupert Lanzenberger, Markus Barth, Amir Reza Tahamtan, Denny Milakara, Andreas Gartus, and Roland Beisteiner. Influence of fmri smoothing procedures on replicability of fine scale motor localization. *NeuroImage*, 24:323–331, 2005.

G. L. Gerstein. *The neurosciences: second study program*, chapter Functional association of neurons: Detection and interpretations, pages 648–661. Rockefeller University Press, 1970.

A.B. Geva and D.H Kerem. Forecasting generalized epileptic seizures from the eeg signal by wavelet analysis and dynamic unsupervised fuzzy clustering. *IEEE Transactions on Biomedical Engineering*, 45:1205–1216, 1998.

Xavier Golay, Spyros Kollias, Gautier Stoll, Dieter Meier, Anton Valavanis, and Dr. Peter Boesiger, Prof. A new correlation-based fuzzy logic clustering algorithm for fmri. *Magnetic Resonance in Medicine*, 40:249–260, 1998.

Heather L. Gordon and Rajmund L. Somorjai. Fuzzy cluster analysis of molecular dynamics trajectories. *Proteins: Structure, Function, and Bioinformatics*, 14:249–264, 1992.

Cyril Goutte, Peter Toft, Egill Rostrup, Finn . Nielsen, and Lars Kai Hansen. On clustering fmri time series. *NeuroImage*, 9:298–310, 1999.

Lars Kai Hansen, Jan Larsen, Finn rup Nielsen, Stephen C. Strother, Egill Rostrup, Robert Savoy, Nicholas Lange, John Sidtis, Claus Svarer, and Olaf B. Paulson. Generalizable patterns in neuroimaging: How many principal components? *NeuroImage*, 9:534–544, 1999.

David J. Heeger, Alex C Huk, Wilson S. Geisler, and Duane G. Albrecht. Spikes versus bold: what does neuroimaging tell us about neuronal activity? *Nature Neuroscience*, 3:631–633, 2000.

Erkki Hkkinen and Pasi Koikkalainen. Som based visualization in data analysis. In *Lecture Notes in Computer Science*, pages 601–606. Springer Berlin / Heidelberg, 1997.

B. Horwitz, K. J. Friston, and J. G. Taylorc. Neural modeling and functional brain imaging: an overview. *Neural Networks*, 13:829–846, 2000.

Barry Horwitz. Data analysis paradigms for metabolic-flow data: Combining neural modeling and functional neuroimaging. *Human Brain Mapping*, 2: 112–122, 1994.

X. Hu, T.H. Le, T. Parrish, and P Erhard. Retrospective estimation and correction of physiological fluctuation in functional mri. *Magn Reson Med*, 34:201–212, 1995.

A. Hyvrinen and E. Oja. Independent component analysis: Algorithms and application. *Neural Networks*, 13:411–430, 2000.

JE Jackson. *A Users Guide to Principal Components*. Wiley-Interscience, 1991.

I.T. Jolliffe. *Principal component analysis*. Springer, 2002.

M. Jueptner and C. Weiller. Does measurement of regional cerebral blood flow reflect synaptic activity? implications for pet and fmri. *Neuroimage*, 2: 148–156, 1995.

T. Jung, S. Makeig, M. Mckeown, A. Bell, T. Lee, and T. Sejnowski. Imaging brain dynamics using independent component analysis. *Proc. IEEE*, 89(7):1107–1122, 2001. URL `http://citeseerx.ist.psu.edu/viewdoc/summary?doi=10.1.1.8.888`.

Teuvo Kohonen. *Self-Organizing Maps*. Springer-Verlag, 1995.

Teuvo Kohonen. The self-organizing map. *Neurocomputing*, 21:1–6, 1998.

Shang-Hong Lai and Ming Fang. A novel local pca-based method for detecting activation signals in fmri. *Magnetic Resonance Imaging*, 17:827–836, 1999.

P. C. Lauterbur. Image formation by induced local interactions: Examples employing nuclear magnetic resonance. *Nature*, 242(5394):190–191, March 1973. doi: 10.1038/242190a0. URL `http://dx.doi.org/10.1038/242190a0`.

Nicole A. Lazar. *The Statistical Analysis of Functional MRI Data*, chapter Noise and Data Preprocessing, pages 37–51. Springer New York, 2008.

N. K. Logothetis. The neural basis of the blood-oxygen-level-dependent functional magnetic resonance imaging signal. *Philos Trans R Soc Lond B Biol Sci*, 357:1003–1037, 2002.

N. K. Logothetis. What we can do and what we cannot do with fmri. *Nature*, 453:869–878, 2008.

Scott Makeig, Tzyy-Ping Jung, Anthony J. Bell, Dara Ghahremani, and Terrence J. Sejnowski. Blind separation of auditory event-related brain responses into independent components. *Neurobiology*, 94:1097910984, 1997.

M Mata, DJ Fink, H Gainer, CB Smith, L Davidsen, H Savaki, WJ Schwartz, and L. Sokoloff. Activity-dependent energy metabolism in rat posterior pituitary primarily reflects sodium pump activity. *Joural of Neurochemistry*, 34:213–215, 1980.

A. R. McIntosh and F. Gonzalez-Lima. Structural equation modeling and its application to network analysis in functional brain imaging. *Human Brain Mapping*, 2:2–22, 1994.

Martin J. McKeown and Terrence J. Sejnowski. Independent component analysis of fmri data: Examining the assumptions. *Human Brain Mapping*, 6: 368–372, 1998.

Martin J. McKeown, Scott Makeig, Greg G. Brown, Tzyy-Ping Jung, Sandra S. Kindermann, Anthony J. Bell, and Terrence J. Sejnowski. Analysis of fmri data by blind separation into independent spatial components. *Human Brain Mapping*, 6:160–188, 1998a.

MJ McKeown, TP Jung, S Makeig, G Brown, SS Kindermann, TW Lee, and TJ. Sejnowski. Spatially independent activity patterns in functional mri data during the stroop color-naming task. *Proc Natl Acad Sci U S A*, 95: 803–810, 1998b.

S. McKie and J. Brittenden. (ii) basic science: magnetic resonance imaging. *Current Orthopaedics*, 19(1):13 – 19, 2005. ISSN 0268-0890. doi: DOI:10.

1016/j.cuor.2005.01.003. URL http://www.sciencedirect.com/science/article/B6WD9-4G002MF-1/2/2b7c9603a6d2eaec0740d953c6c192d0.

Chad H. Moritz, Victor M. Haughtona, Dietmar Cordesa, Michelle Quigleya, and M. Elizabeth Meyeranda. Whole-brain functional mr imaging activation from a finger-tapping task examined with independent component analysis. *American Journal of Neuroradiology*, 21:1629–1635, 2000.

A. Mosso. *Ueber den Kreislauf des Blutes im Menschlichen Gehirn*. Verlag von Veit & Company, 1881.

F. Murtagh. Interpreting the kohonen self-organizing feature map using contiguity-constrained clustering. *Pattern Recognition Letters*, 16:399–408, 1995.

Shing-Chung Ngan and Xiaoping Hu. Analysis of functional magnetic resonance imaging data using self-organizing mapping with spatial connectivity. *Magnetic Resonance in Medicine*, 41:936–946, 1999.

S. Ogawa, T. M. Lee, A. R. Kay, and D. W. Tank. Brain magnetic resonance imaging with contrast dependent on blood oxygenation. *Proceedings of the National Academy of Sciences of the United States of America*, 87(24):9868–9872, December 1990a. ISSN 0027-8424. doi: 10.1073/pnas.87.24.9868. URL http://dx.doi.org/10.1073/pnas.87.24.9868.

S. Ogawa, T. S. Lee, A. S. Nayak, and P. Glynn. Oxygenation-sensitive contrast in magnetic resonance image of rodent brain at high magnetic fields. *Magnetic Resonance in Medicine*, 26:68–78, 1990b.

E. Oja. Neural networks, principal components, and subspaces. *International Journal of Neural Systems*, 1:61–68, 1989.

L. Pauling and C.D Coryell. The magnetic properties and structure of hemoglobin, oxyhemoglobin and carbonmonoxyhemoglobin. *Proc. Natl. Acad. Sci. U. S. A*, 22:210–216, 1936.

Judea Pearl. Causal inference in the health sciences: A conceptual introduction. *Health Services and Outcomes Research Methodology*, 2:189–220, 2001.

SJ Peltier, TA Polk, and DC Noll. Detecting low-frequency functional connectivity in fmri using a self-organizing map (som) algorithm. *Hum Brain Mapping*, 20:220–226, 2003.

MI Posner, SE Petersen, PT Fox, and ME Raichle. Localization of cognitive operations in the human brain. *Science*, 240:1627–1631, 1998.

E. M. Purcell, H. C. Torrey, and R. V. Pound. Resonance absorption by nuclear magnetic moments in a solid. *Phys. Rev.*, 69:37–38, 1946.

M. Raichle. A brief history of human brain mapping. *Trends in Neurosciences*, 32:118–126, December 2008. ISSN 01662236. doi: 10.1016/j.tins.2008.11.001. URL `http://dx.doi.org/10.1016/j.tins.2008.11.001`.

M. E. Raichle and M. A. Mintun. Brain work and brain imaging. *Annu Rev Neurosci*, 29:449–476, 2006. ISSN 0147-006X. doi: 10.1146/annurev.neuro.29.051605.112819. URL `http://dx.doi.org/10.1146/annurev.neuro.29.051605.112819`.

B. R. Rosen, R. L. Buckner, and A. M. Dale. Event-related functional mri: Past, present, and future. *Proceedings of the National Academy of Sciences of the United States of America*, 95:773–780, 1998.

C. S. Roy and C. S. Sherrington. On the regulation of the blood-supply of the brain. *The Journal of Physiology*, 11(1-2):85–158, 1890. URL `http://jp.physoc.org/content/11/1-2/85.short`.

Catarina Saiote, Joana Silva, Carlos Gomes, Martin Lauterbach, Sofia Reimo, and Patricia Figueiredo. Parametric fmri correlates of faces at multiple orientations.

Mark J. Sands and Abraham Levitin. Basics of magnetic resonance imaging. *Seminars in Vascular Surgery*, 17(2):66 – 82, 2004. ISSN 0895-7967. doi: DOI:10.1053/j.semvascsurg.2004.03.011. URL `http://www.sciencedirect.com/science/article/B75M4-4CHGDY6-3/2/8cb12d2ca057e377a3201ed0d223f9d2`. Imaging for the Vascular Surgeon.

Gordon B. Scarth, M. McIntyre, B. Wowk, and Ray L. Somorjai. Detection of novelty in functional images using fuzzy clustering. In *Proceedings of the Society of Magnetic Resonance and the European Society For Magnetic Resonance Medicine And Biology, Nice, France, August 19–25, 1995*, 1995.

Friedrich T. Sommer and Andrzej Wichert, editors. *Exploratory analysis and data modeling in functional neuroimaging*. MIT Press, 2003.

Ray L. Somorjai, MarkExploratory analysis Jarmasz, and data modeling in functional neuroimaging. Exploratory analysis of fmri data by fuzzy clustering: philosophy, strategy, tactics, implementation. In *Exploratory analysis and data modeling in functional neuroimaging*. MIT Press, 2003.

Christoph Stippich. *Clinical Functional MRI: Presurgical Functional Neuroimaging*. Springer, 2007.

H N Suma and S Murali. Principal component analysis for analysis and classification of fmri activation maps. *International Journal of Computer Science and Network Security*, 7:235–242, 2007.

Robert-Jan M. van Geuns, Piotr A. Wielopolski, Hein G. de Bruin, Benno J. Rensing, Peter M.A. van Ooijen, Marc Hulshoff, Matthijs Oudkerk, and Pim J. de Feyter. Basic principles of magnetic resonance imaging. *Progress in Cardiovascular Diseases*, 42(2):149 – 156, 1999. ISSN 0033-0620. doi: DOI:10.1016/S0033-0620(99)70014-9. URL `http://www.sciencedirect.com/science/article/B75BG-4HGNR2C-3/2/e4af765ae3c8cdcce8a550623818e055`. Advances in Coronary Imaging.

Arno Villringer, Bruce R. Rosen, John W. Belliveau, Jerome L. Ackerman, Randall B. Lauffer, Richard B. Buxton, Yong-Sheng Chao, Van J. Wedeenand, and Thomas J. Brady. Dynamic imaging with lanthanide chelates in normal brain: Contrast due to magnetic susceptibility effects. *Magnetic Resonance in Medicine*, 6:164–174, 1988.

Roberto Viviani, Georg Gron, and Manfred Spitzer. Functional principal component analysis of fmri data. *Human Brain Mapping*, 24:109–129, 2005.

L Zambreanu, RG Wise, JC Brooks, GD Iannetti, and Tracey I. A role for the brainstem in central sensitisation in humans. evidence from functional magnetic resonance imaging. *Pain*, 3:397–407, 2005.

S. Zeki. *Signal and Sense*, chapter Functional specialization in the visual cortex: the generation of separate constructs and their multistage integration, pages 85–130. Wiley, 1990.